Computers and Mathematics with Applications 70 (2015) 2454–2473

Contents lists available at ScienceDirect

Computers and Mathematics with Applications

journal homepage: www.elsevier.com/locate/camwa

Analysis and computation of the elastic wave equation with random coefficients

Mohammad Motamed [a,*], Fabio Nobile [b], Raúl Tempone [c]

[a] Department of Mathematics and Statistics, The University of New Mexico, Albuquerque, NM 87131, USA
[b] MATHICSE-CSQI, École Polytechnique Fédérale de Lausanne, Lausanne, Switzerland
[c] King Abdullah University of Science and Technology, Jeddah, Saudi Arabia

ARTICLE INFO

Article history:
Received 23 August 2014
Received in revised form 6 September 2015
Accepted 12 September 2015
Available online 9 October 2015

Keywords:
Uncertainty quantification
Stochastic partial differential equations
Elastic wave equation
Collocation method
Error analysis

ABSTRACT

We consider the stochastic initial–boundary value problem for the elastic wave equation with random coefficients and deterministic data. We propose a stochastic collocation method for computing statistical moments of the solution or statistics of some given quantities of interest. We study the convergence rate of the error in the stochastic collocation method. In particular, we show that, the rate of convergence depends on the regularity of the solution or the quantity of interest in the stochastic space, which is in turn related to the regularity of the deterministic data in the physical space and the type of the quantity of interest. We demonstrate that a fast rate of convergence is possible in two cases: for the elastic wave solutions with high regular data; and for some high regular quantities of interest even in the presence of low regular data. We perform numerical examples, including a simplified earthquake, which confirm the analysis and show that the collocation method is a valid alternative to the more traditional Monte Carlo sampling method for approximating quantities with high stochastic regularity.

Published by Elsevier Ltd.

1. Introduction

The elastic wave equation describes phenomena such as seismic waves in the earth and ultrasound waves in elastic materials. It is a system of linear second order hyperbolic partial differential equations (PDEs) in a two or three dimensional physical space and has a more complex form than the standard acoustic wave equation, as it accounts for both longitudinal and transverse motions. There can also be surface waves traveling along a free surface, as well as waves that travel along internal material discontinuities.

It is often desirable to include uncertainty in the PDE models and quantify its effects on the predicted solution or other quantities of physical interest. The uncertainty may be either due to the lack of knowledge (systematic uncertainty), or due to inherent variations of the physical system (statistical uncertainty). In earthquake modeling, for instance, seismic waves propagate in a geological region where, due to soil spatial variability and the uncertainty of measured soil parameters, both kinds of uncertainties are present.

Probability theory provides an effective tool to describe and propagate uncertainty. It parametrizes the uncertain input data either in terms of a finite number of random variables or more generally by random fields. Several techniques are available for solving PDEs in probabilistic setting. The most frequently used technique is the Monte Carlo sampling which

* Corresponding author.
E-mail addresses: motamed@math.unm.edu (M. Motamed), fabio.nobile@epfl.ch (F. Nobile), raul.tempone@kaust.edu.sa (R. Tempone).

http://dx.doi.org/10.1016/j.camwa.2015.09.013
0898-1221/Published by Elsevier Ltd.

features a very slow convergence rate, see e.g. [1]. The slow convergence of Monte Carlo can be improved by quasi Monte Carlo (see, e.g., [2]) and multi-level Monte Carlo (see, e.g., [3]) techniques. Other recent approaches, which in certain situations feature a much faster convergence rate, include Stochastic Galerkin [4–8] and Stochastic Collocation [9–12]. Such methods are based on global polynomials and exploit the possible regularity that the solution might have with respect to the input parameters to yield a very fast convergence.

For stochastic elliptic and parabolic problems, under particular assumptions, the solution is analytic with respect to the input random parameters [9,13,14]. Consequently, Stochastic Galerkin and Stochastic Collocation methods can be successfully applied to such problems due to the fast decay of the error as a result of the high stochastic regularity. For stochastic hyperbolic problems, the regularity analysis is more involved. For the one-dimensional scalar advection equation with a time- and space-independent random wave speed, it is shown that the solution possess high regularity provided the data live in suitable spaces [15–17]. The main difficulty, however, arises when the coefficients vary in space or time. Recently, in [18], we have studied the second order acoustic wave equation with discontinuous random wave speeds. We have shown that unlike in elliptic and parabolic problems, the solution to hyperbolic problems is not in general analytic with respect to the random variables. Therefore, the rate of convergence may only be algebraic. However, a fast rate of convergence is still possible for some quantities of interest and for the wave solution with particular types of data. For the more difficult case of stochastic nonlinear conservation laws, where the corresponding regularity theory is lacking, we refer to the computational studies in [19–23].

In this work, we consider the elastic wave equation in a random heterogeneous medium with time-independent and smooth material properties, augmented with deterministic initial data and source terms and subject to homogeneous Neumann or Dirichlet boundary conditions. Since the analysis of hyperbolic problems with non-homogeneous boundary conditions and general boundary data is very complicated and not well developed (see [24,25] for the analysis for particular types of boundary conditions), we assume that the initial data and external forcing are compactly supported inside the domain and that the wave solution does not reach the boundary. In the numerical tests however, we employ absorbing boundary conditions and study the general case where the wave solutions can reach the boundary. Moreover, we are mainly interested in low-to-moderate frequency seismic waves propagating in slowly varying underlying media. Therefore we further assume that the wave length is not very small compared to the overall size of the domain and is comparable to the scale of the variations in the medium (see [26], where we consider multiscale elastic problems in highly varying media). We study the well-posedness and stochastic regularity of the problem by employing the energy method, which is based on the weak formulation of the problem and integration by parts. The main results of this paper, presented in Theorems 3, 4, 5, 6, is that the regularity of the solution or the quantity of interest in the stochastic space is closely related to the regularity of the deterministic data in the physical space and the type of the quantity of interest. We demonstrate that high stochastic regularity is possible in two cases: for the elastic wave solutions with high regular data; and for some high regular physical quantities of interest even in the presence of low regular data. For such problems, a fast spectral convergence is therefore possible when a stochastic collocation method is employed. We note that the stochastic collocation technique presented here is not new and has been widely used for the uncertainty propagation of many PDE models, see e.g. [9–12]. Here, we have adapted and employed the method to compute the statistics of the solution and QoIs and verify the regularity results obtained in the paper. The main contribution of this paper on the computational side is the inclusion of the filtering technique in the stochastic collocation algorithm. By introducing a low-pass filter, we add extra stochastic regularity, which in turn reduces the stochastic collocation error, as shown in this paper. We note that this will also introduce an extra filtering error. However, the filtering error can be suppressed by the collocation error if the filter parameters are properly chosen. A rigorous error analysis for the filtered quantities and the optimal choice of filter parameters will be studied in future works. We refer to [26] which – motivated by the present paper – studies the filtering technique in more details and presents some preliminary results.

This paper contributes to both *analysis* and *computation* of wave propagation problems subject to uncertainty. The main contributions include: (1) Extension of our work [18] to hyperbolic systems with vector-valued solutions; (2) Rigorous well-posedness and stochastic regularity analysis for the wave solution and mollified and filtered QoIs under general assumptions on the data, which is not discussed in other works; and (3) Application of the stochastic collocation method together with filtering techniques to seismic wave problems.

The outline of the paper is as follows. In Section 2 we formulate the mathematical problem and establish the main assumptions. The well-posedness of the problem is studied in Section 3. In Section 4, we provide regularity results on the solution and some physical quantities of interest. The collocation method for solving the underlying stochastic PDE and the related error convergence results are addressed in Section 5. In Section 6 we perform some numerical examples. Finally, we present our conclusions in Section 7.

2. Problem statement

Let D be an open bounded subset of $\mathbb{R}^d$, $d = 2, 3$, with a smooth boundary ∂D, and $(\Omega, \mathcal{F}, P)$ be a complete probability space. Here, Ω is the set of outcomes, $\mathcal{F} \subset 2^\Omega$ is the σ-algebra of events and $P : \mathcal{F} \to [0, 1]$ is a probability measure. Consider the stochastic initial–boundary value problem (IBVP): find a random vector-valued function $\mathbf{u} : [0, T] \times \bar{D} \times \Omega \to \mathbb{R}^d$, such that P-almost everywhere in Ω, i.e. almost surely (a.s), the following holds:

$$\nu(\mathbf{x}, \omega)\, \mathbf{u}_{tt}(t, \mathbf{x}, \omega) - \nabla \cdot \boldsymbol{\sigma}(\mathbf{u}(t, \mathbf{x}, \omega)) = \mathbf{f}(t, \mathbf{x}) \quad \text{in } [0, T] \times D \times \Omega, \tag{1a}$$

$$\mathbf{u}(0,\mathbf{x},\omega)=\mathbf{g}_1(\mathbf{x}),\qquad \mathbf{u}_t(0,\mathbf{x},\omega)=\mathbf{g}_2(\mathbf{x})\qquad \text{on } \{t=0\}\times D\times\Omega, \tag{1b}$$

$$\boldsymbol{\sigma}(\mathbf{u}(t,\mathbf{x},\omega))\cdot\hat{\mathbf{n}}=\mathbf{0}\qquad \text{on } [0,T]\times\partial D\times\Omega. \tag{1c}$$

Here, the stress tensor is

$$\boldsymbol{\sigma}(\mathbf{u})=\lambda(\mathbf{x},\omega)\,\nabla\cdot\mathbf{u}\,I+\mu(\mathbf{x},\omega)\,(\nabla\mathbf{u}+(\nabla\mathbf{u})^{\top}), \tag{2}$$

where $\mathbf{u}=(u_1,\ldots,u_d)^{\top}$ is the displacement vector, t and $\mathbf{x}=(x_1,\ldots,x_d)^{\top}$ are the time and location, respectively, and I is the identity matrix. A homogeneous Neumann (or stress-free) boundary condition (1c) is imposed on the boundary ∂D, where $\hat{\mathbf{n}}$ is the outward unit normal to the boundary ∂D.

In this section, we take the external forcing and initial data as

$$\mathbf{f}\in\mathbf{L}^2((0,T);\mathbf{L}^2(D)),\qquad \mathbf{g}_1\in\mathbf{H}^1(D),\qquad \mathbf{g}_2\in\mathbf{L}^2(D). \tag{3}$$

The precise definition of the above real vector-valued function spaces will be given in Section 3. More general assumptions on the regularity of data will be given in Section 4, where we consider both weaker and stronger assumptions, see (15).

Throughout this paper, we assume that the initial data and external forcing are compactly supported inside D and that the final time T and the domain D are selected so that the wave solution $\mathbf{u}$ does not reach the boundary ∂D. Hence the displacement vector $\mathbf{u}$ will remain zero on the boundary for all $t\in[0,T]$ almost surely. Consequently, instead of the homogeneous Neumann boundary condition (1c), we can also consider a homogeneous Dirichlet boundary condition

$$\mathbf{u}(t,\mathbf{x},\omega)=\mathbf{0}\quad \text{on } [0,T]\times\partial D\times\Omega. \tag{4}$$

These assumptions will simplify the treatment of boundary conditions and the analysis in the physical space. In particular, the same regularity results will hold for the initial value problem (1a)–(1b) both in the whole space $\mathbb{R}^d$ (Cauchy problem) and in the bounded domain D augmented with either (1c) or (4). We will then concentrate on the analysis in the stochastic (or parameter) space and present a rigorous stochastic regularity analysis, based on which the convergence rate of the stochastic collocation method is obtained. Other types of boundary conditions, including non-homogeneous Dirichlet, non-homogeneous Neumann, and absorbing boundary conditions, will be briefly addressed in Section 3.3. A rigorous treatment of such more general boundary conditions are the subject of our current work and will be presented elsewhere.

The material properties are characterized by the density ν and the Lamé parameters λ and μ that define the stress tensor (2). We consider a heterogeneous medium and assume that these parameters are random and $\mathbf{x}$-smooth, i.e.,

$$\nu(.,\omega),\ \ \lambda(.,\omega),\ \ \mu(.,\omega)\in C^{\infty}(D),\quad \text{a.s.} \tag{5}$$

This regularity may be relaxed, see for instance Remark 3. We also assume that the parameters are uniformly bounded and coercive, and therefore the following inequalities hold:

$$0<\nu_{\min}\le\nu(\mathbf{x},\omega)\le\nu_{\max}<\infty,\quad \forall\,\mathbf{x}\in D,\quad \text{a.s,} \tag{6a}$$

$$0<\lambda_{\min}\le\lambda(\mathbf{x},\omega)\le\lambda_{\max}<\infty,\quad \forall\,\mathbf{x}\in D,\quad \text{a.s,} \tag{6b}$$

$$0<\mu_{\min}\le\mu(\mathbf{x},\omega)\le\mu_{\max}<\infty,\quad \forall\,\mathbf{x}\in D,\quad \text{a.s.} \tag{6c}$$

We note that using a similar approach to [9,27,28] we can also treat the case of parameters with non-uniform elliptic properties by considering random lower and upper bounds for the parameters in assumption (6), i.e. for example $\nu_{\min}=\nu_{\min}(\omega)$ and $\nu_{\max}=\nu_{\max}(\omega)$. We can then carry out the proofs point-wise in ω, under proper bounded moment assumptions on $\nu_{\min}^{-1}$ and $\nu_{\max}$. The effect of loss of coercivity on the stochastic collocation method has been further analyzed in [18]. In this paper we consider only uniform elliptic property (6). The system (1) admits longitudinal (P or pressure) and transverse (S or shear) waves which, in the case of constant density, propagate at phase velocities $c_p=\sqrt{(2\,\mu+\lambda)/\nu}$, and $c_s=\sqrt{\mu/\nu}$, respectively. There can also be surface waves traveling along a free surface, as well as waves that travel along internal material discontinuities. We note that the uniform ellipticity assumption (6) often holds and is practical in wave propagation problems, since the wave speeds are uniformly bounded from below and above in compressible materials.

We further make the following *finite dimensional noise* assumption on the form of the coefficients,

$$\nu(\mathbf{x},\omega)=\nu(\mathbf{x},Y_1(\omega),\ldots,Y_N(\omega)),\quad \forall\,\mathbf{x}\in D,\quad \text{a.s,} \tag{7a}$$

$$\lambda(\mathbf{x},\omega)=\lambda(\mathbf{x},Y_1(\omega),\ldots,Y_N(\omega)),\quad \forall\,\mathbf{x}\in D,\quad \text{a.s,} \tag{7b}$$

$$\mu(\mathbf{x},\omega)=\mu(\mathbf{x},Y_1(\omega),\ldots,Y_N(\omega)),\quad \forall\,\mathbf{x}\in D,\quad \text{a.s,} \tag{7c}$$

where $N\in\mathbb{N}_+$ and $Y=[Y_1,\ldots,Y_N]\in\mathbb{R}^N$ is a random vector. We denote by $\Gamma_n\equiv Y_n(\Omega)$ the image of each component Y_n and assume that Y_n is bounded for $n=1,\ldots,N$. We let $\Gamma=\prod_{n=1}^{N}\Gamma_n$ and assume further that the random vector Y has a bounded joint probability density function $\rho:\Gamma\to\mathbb{R}_+$ with $\rho\in L^{\infty}(\Gamma)$. In the present work, we only consider a small number of random variables N. The case of white noise random fields or when the number of random variables is very large ($N\to\infty$) is out of the scope of this paper and needs further investigations.

The finite dimensional noise assumption implies that the solution of the stochastic IBVP (1) can be described by only N random variables,

$$\mathbf{u}(t,\mathbf{x},\omega)=\mathbf{u}(t,\mathbf{x},Y_1(\omega),\ldots,Y_N(\omega)).$$

This turns the original stochastic problem into a deterministic IBVP for the elastic wave equation with an N-dimensional parameter, which allows the use of standard finite difference and finite element methods to approximate the solution of the resulting deterministic problem $\mathbf{u} = \mathbf{u}(t, \mathbf{x}, Y)$, where $t \in [0, T]$, $\mathbf{x} \in D$, and $Y \in \Gamma$. Note that the knowledge of $\mathbf{u} = \mathbf{u}(t, \mathbf{x}, Y)$ fully determines the law of the random field $\mathbf{u} = \mathbf{u}(t, \mathbf{x}, \omega)$. The ultimate goal is then the prediction of statistical moments of the solution or statistics of some given quantities of physical interest.

In this work, we consider $\mathbf{x}$-smooth random parameters (5) with bounded mixed Y-derivatives of any order. Therefore, for a multi-index $\mathbf{k} \in \mathbb{N}^N$ with $|\mathbf{k}| \geq 0$, we assume

$$\|\partial_Y^{\mathbf{k}} \nu\|_{L^\infty(D)}, \ \|\partial_Y^{\mathbf{k}} \lambda\|_{L^\infty(D)}, \ \|\partial_Y^{\mathbf{k}} \mu\|_{L^\infty(D)} < \infty, \quad \forall\, Y \in \Gamma. \tag{8}$$

For instance, the random coefficients may be given linearly in Y by

$$\nu(\mathbf{x}, \omega) = \hat{\nu}_0(\mathbf{x}) + \sum_{n=1}^{N} \hat{\nu}_n(\mathbf{x})\, Y_n(\omega), \tag{9a}$$

$$\lambda(\mathbf{x}, \omega) = \hat{\lambda}_0(\mathbf{x}) + \sum_{n=1}^{N} \hat{\lambda}_n(\mathbf{x})\, Y_n(\omega), \tag{9b}$$

$$\mu(\mathbf{x}, \omega) = \hat{\mu}_0(\mathbf{x}) + \sum_{n=1}^{N} \hat{\mu}_n(\mathbf{x})\, Y_n(\omega), \tag{9c}$$

where $\hat{\nu}_i$, $\hat{\lambda}_i$ and $\hat{\mu}_i$, with $i = 0, 1, \ldots, N$, are smooth functions defined everywhere in D, and Y_n are independent and identically distributed random variables. A typical example is when the random field $\nu(\mathbf{x}, \omega)$ is approximated by a truncated Karhunen–Loéve expansion with N terms. We note that, in this case, the covariance function should be such that the corresponding eigenfunctions are smooth. We also notice that (9) together with (6) imply that random variables Y_n are bounded. For simplicity, and without loss of generality, the proof of regularity results in the stochastic space are given for linear coefficients (9). However, we emphasize that the important assumption here is (8). The regularity results hold true for general coefficients satisfying (5)–(8), see Remark 2. We will address the cases of discontinuous and piecewise $\mathbf{x}$-smooth random parameters elsewhere. See also our work in [18] on the acoustic wave equation with discontinuous random coefficients.

3. Well-posedness

The well-posedness theory of linear hyperbolic IBVPs is well developed for many classes of first and second order systems with different types of non-homogeneous boundary conditions, including Dirichlet, Neumann, Robin, and absorbing-type boundary conditions involving time derivatives. This general theory is based on a variety of mathematical techniques, such as the energy integral method, Laplace–Fourier transform, the construction of symmetrizers, and the theory of pseudo-differential operators (see,e.g., [29–32,25]).

In this section, we will address the well-posedness of the stochastic IBVP (1) with the data satisfying (3) and the coefficients satisfying (5)–(7).

3.1. Function spaces

We first define function spaces that we need in this work. For a real vector-valued function $\mathbf{v}(Y) = (v_1(Y), \ldots, v_d(Y))^\top \in \mathbb{R}^d$ of the random vector $Y \in \Gamma$, we define the space of square integrable functions:

$$\mathbf{L}^2_\rho(\Gamma) = \left\{ \mathbf{v} : \Gamma \to \mathbb{R}^d, \ \int_\Gamma \sum_{i=1}^{d} |v_i(Y)|^2\, \rho(Y)\, dY < \infty \right\},$$

endowed with the inner product

$$(\mathbf{v}, \mathbf{u})_{L^2_\rho(\Gamma)} = \sum_{i=1}^{d} \mathbb{E}\,[v_i\, u_i] = \int_\Gamma \sum_{i=1}^{d} v_i\, u_i\, \rho(Y)\, dY.$$

For a real vector-valued function $\mathbf{v}(\mathbf{x}) \in \mathbb{R}^d$ of $\mathbf{x} \in D$, we define the Sobolev space $\mathbf{H}^k(D)$ for integer order $k \geq 0$:

$$\mathbf{H}^k(D) = \left\{ \mathbf{v} : D \to \mathbb{R}^d, \int_D \sum_{i=1}^{d} |\partial_{\mathbf{x}}^\alpha v_i(\mathbf{x})|^2\, d\mathbf{x} < \infty, \ \forall \alpha, \ |\alpha| \leq k \right\},$$

where $\alpha = (\alpha_1, \ldots, \alpha_d) \in \mathbb{Z}^d_+$ is a multi-index with $|\alpha| = \alpha_1 + \cdots + \alpha_d$, and $\partial_{\mathbf{x}}^\alpha := \frac{\partial^{|\alpha|}}{\partial_{x_1}^{\alpha_1} \ldots \partial_{x_d}^{\alpha_d}}$. Naturally, $\mathbf{H}^k(D)$ is a Hilbert space with the inner product

$$(\mathbf{v}, \mathbf{u})_{\mathbf{H}^k(D)} = \int_D \sum_{|\alpha| \leq k} \sum_{i=1}^{d} \partial_{\mathbf{x}}^\alpha v_i(\mathbf{x})\, \partial_{\mathbf{x}}^\alpha u_i(\mathbf{x})\, d\mathbf{x}.$$

For the particular case of $k = 0$, we obtain the space of square integrable vector-valued functions $\mathbf{L}^2(D) = \mathbf{H}^0(D)$. The space $\mathbf{H}^{-k}(D)$ is the dual of $\mathbf{H}^k(D)$. We also define the space $\mathbf{H}_0^k(D)$ as the closure of the space of smooth functions with compact support $\mathbf{C}_0^\infty(D)$ in $\mathbf{H}^k(D)$.

Now let $\mathbf{H}^k(D) \otimes \mathbf{L}^2_\rho(\Gamma)$ be a tensor space with tensor inner product

$$(\mathbf{v}, \mathbf{u})_{\mathbf{H}^k(D)\otimes\mathbf{L}^2_\rho(\Gamma)} = \int_\Gamma \int_D \sum_{|\alpha|\le k} \sum_{i=1}^{d} \partial_{\mathbf{x}}^\alpha v_i(\mathbf{x})\, \partial_{\mathbf{x}}^\alpha u_i(\mathbf{x})\, d\mathbf{x}\, \rho(Y)\, dY.$$

Thus, if $\mathbf{v} \in \mathbf{H}^k(D) \otimes \mathbf{L}^2_\rho(\Gamma)$, then $\mathbf{v}(\mathbf{x}, .) \in \mathbf{L}^2_\rho(\Gamma)$ a.e. on D and $\mathbf{v}(., Y) \in \mathbf{H}^k(D)$ a.e. on Γ. We then introduce the mapping $\mathbf{u} : [0, T] \to \mathbf{H}^k(D) \otimes \mathbf{L}^2_\rho(\Gamma)$, defined by

$$[\mathbf{u}(t)](\mathbf{x}, Y) := \mathbf{u}(t, \mathbf{x}, Y), \quad \forall\, t \in [0, T],\ \mathbf{x} \in D,\ Y \in \Gamma.$$

In other words, we view the function $\mathbf{u}(t, \mathbf{x}, Y)$ as a function of t with values $\mathbf{u}(t)$ in the Hilbert space $\mathbf{H}^k(D) \otimes \mathbf{L}^2_\rho(\Gamma)$. Similarly, we introduce the function $\mathbf{f} : [0, T] \to \mathbf{H}^k(D)$, defined by

$$[\mathbf{f}(t)](\mathbf{x}) := \mathbf{f}(t, \mathbf{x}), \quad \forall\, t \in [0, T],\ \mathbf{x} \in D.$$

Finally, for a real Hilbert space $\mathbf{H}^k(D)$ equipped with the norm $\|\mathbf{v}\|_{\mathbf{H}^k(D)} = (\mathbf{v}, \mathbf{v})^{1/2}_{\mathbf{H}^k(D)}$, we introduce the time-involving space $\mathbf{L}^2((0, T); \mathbf{H}^k(D) \otimes \mathbf{L}^2_\rho(\Gamma))$, consisting of all measurable vector-valued functions $\mathbf{v}$ with $\int_{[0,T]\times\Gamma} \|\mathbf{v}\|^2_{\mathbf{H}^k(D)}\, \rho(Y)\, dY\, dt < \infty$. Similarly, for the Hilbert space $\mathbf{V} = \mathbf{H}^k(D) \otimes \mathbf{L}^2_\rho(\Gamma)$, we denote by $\mathbf{C}^m([0, T]; \mathbf{V})$, with $m = 0, 1, \ldots$, the space of all m times continuously differentiable functions defined on $[0, T]$ with values in $\mathbf{V}$.

3.2. Weak formulation

Due to assumption (3) on the data, we need to consider the weak formulation of the problem (1),

$$\int_{[0,T]\times D\times\Gamma} \left(\nu\, \mathbf{u}'' \cdot \mathbf{v} + \nabla\mathbf{v} : \boldsymbol{\sigma}(\mathbf{u})\right)\, \rho\, dY\, d\mathbf{x}\, dt = \int_{[0,T]\times D\times\Gamma} \mathbf{f} \cdot \mathbf{v}\, \rho\, dY\, d\mathbf{x}\, dt, \tag{10}$$

for all test functions $\mathbf{v} \in \mathbf{C}_0^\infty([0, T]; \mathbf{H}^1(D) \otimes \mathbf{L}^2_\rho(\Gamma))$, thanks to integration by parts and (1c). Here, the tensor contraction on tensors A and B is defined by $A : B = \sum_{i,j} A_{ij} B_{ij}$. We now define the notion of weak solutions to (1) under the assumption (3).

Definition 1. For the stochastic IBVP (1) with the data satisfying (3) and the coefficients satisfying (5)–(7), the function $\mathbf{u} \in \mathbf{L}^2((0, T); \mathbf{H}^1(D) \otimes \mathbf{L}^2_\rho(\Gamma))$ with $\mathbf{u}' \in \mathbf{L}^2((0, T); \mathbf{L}^2(D) \otimes \mathbf{L}^2_\rho(\Gamma))$ and $\mathbf{u}'' \in \mathbf{L}^2((0, T); \mathbf{H}^{-1}(D) \otimes \mathbf{L}^2_\rho(\Gamma))$ is a weak solution provided the following hold:

(i) $\mathbf{u}(0) = \mathbf{g}_1$ and $\mathbf{u}'(0) = \mathbf{g}_2$,
(ii) for all test functions $\mathbf{v} \in \mathbf{C}_0^\infty([0, T]; \mathbf{H}^1(D) \otimes \mathbf{L}^2_\rho(\Gamma))$, the weak formula (10) holds.

Note that since $\mathbf{u}'' \in \mathbf{L}^2((0, T); \mathbf{H}^{-1}(D) \otimes \mathbf{L}^2_\rho(\Gamma))$, then $\mathbf{u}' \in \mathbf{H}^1((0, T); \mathbf{H}^{-1}(D) \otimes \mathbf{L}^2_\rho(\Gamma))$ and therefore $\mathbf{u}' \in \mathbf{C}^0([0, T]; \mathbf{H}^{-1}(D) \otimes \mathbf{L}^2_\rho(\Gamma))$, see Theorem 5 in Section 5.9.2 in [33]. Similarly, we have $\mathbf{u} \in \mathbf{C}^0([0, T]; \mathbf{L}^2(D) \otimes \mathbf{L}^2_\rho(\Gamma))$. Therefore, $\mathbf{u}(0)$ and $\mathbf{u}'(0)$ in (i) are well-defined. We note that, due to (2), we have $\nabla\mathbf{v} : \boldsymbol{\sigma}(\mathbf{u}) = \lambda\, (\nabla \cdot \mathbf{v})\, (\nabla \cdot \mathbf{u}) + \mu\, \nabla\mathbf{v} : (\nabla\mathbf{u} + (\nabla\mathbf{u})^\top)$.

We have the following result on the existence and uniqueness of the weak solution.

Theorem 1. *Consider the Stochastic IBVP (1) with data satisfying (3) and random parameters satisfying (5), (6), and (7). There exists a unique weak solution* $\mathbf{u} \in \mathbf{C}^0([0, T]; \mathbf{H}^1(D) \otimes \mathbf{L}^2_\rho(\Gamma)) \cap \mathbf{C}^1([0, T]; \mathbf{L}^2(D) \otimes \mathbf{L}^2_\rho(\Gamma)) \cap \mathbf{H}^2((0, T); \mathbf{H}^{-1}(D) \otimes \mathbf{L}^2_\rho(\Gamma))$ *to the problem which depends continuously on the data. Moreover, the same result holds when the boundary condition (1c) is replaced by (4).*

Proof. The proof is an easy extension of the proof for deterministic problems, see e.g [30,32]. □

Remark 1. A similar result as in Theorem 1 can be obtained pointwise in $Y \in \Gamma$. In this case we interpret the solution $\mathbf{u}(t, \mathbf{x}, Y)$ as a Hilbert-valued function on Γ,

$$\mathbf{u} = \mathbf{u}(Y) : \Gamma \to \mathbf{C}^0([0, T]; \mathbf{H}^1(D)) \cap \mathbf{C}^1([0, T]; \mathbf{L}^2(D)) \cap \mathbf{H}^2((0, T); \mathbf{H}^{-1}(D)). \tag{11}$$

Such function is uniformly bounded on Γ thanks to assumptions (6). We will use such results in Section 4, where more general assumptions on the data are made.

3.3. Boundary conditions

So far, we have considered the homogeneous Neumann boundary condition (1c). Similar analysis can also be carried on for the homogeneous Dirichlet condition (4). We now briefly address three other types of boundary conditions.

3.3.1. Non-homogeneous Dirichlet boundary conditions

Consider the stochastic IBVP (1) with the boundary condition (1c) replaced by

$$\mathbf{u}(t,\mathbf{x},\omega) = \mathbf{h}_D(t,\mathbf{x}) \quad \text{on } [0,T]\times\partial D\times\Omega, \tag{12}$$

with $\mathbf{h}_D \in \mathbf{L}^2((0,T);\mathbf{H}^1(\partial D))$. By an easy extension of the proof of Theorem 24.1.1 in [32] we can show that Theorem 1 also holds for the stochastic problem (1a)–(1b) with the boundary condition (12). We note that the analysis of the general case $\mathbf{h}_D \in \mathbf{H}^{s_1}((0,T);\mathbf{H}^{s_2}(\partial D))$, with $s_1, s_2 \in \mathbb{R}$, is not yet studied to the best of our knowledge.

3.3.2. Non-homogeneous Neumann boundary conditions

Now consider the stochastic IBVP (1) with the boundary condition (1c) replaced by

$$\boldsymbol{\sigma}(\mathbf{u}(t,\mathbf{x},\omega))\cdot\hat{\mathbf{n}} = \mathbf{h}_N(t,\mathbf{x}) \quad \text{on } [0,T]\times\partial D\times\Omega, \tag{13}$$

with $\mathbf{h}_N \in \mathbf{L}^2((0,T);\mathbf{H}^{1/2}(\partial D))$. Using integration by parts, we obtain (10) with an extra boundary term $\int_{[0,T]\times\partial D\times\Gamma}\mathbf{v}\cdot\boldsymbol{\sigma}(\mathbf{u})\cdot\hat{\mathbf{n}}\ \rho\,dY\,d\mathbf{x}\,dt$ on the right hand side. We first notice that $\boldsymbol{\sigma}(\mathbf{u})\cdot\hat{\mathbf{n}}$ is well-defined on the boundary ∂D, see Appendix B.2 of [32,34]. For instance, in $\mathbb{R}^2$, the domain D may locally be considered as the half-plane $\mathbb{R}^2_0 = \{\mathbf{x} = (x_1,x_2)^\top : x_2 \geq 0, -\infty < x_1 < \infty\}$ with the boundary $\partial D = \{x_2 = 0\}$, for which $\hat{\mathbf{n}} = [0,-1]^\top$. Then, one can show that $\boldsymbol{\sigma}(\mathbf{u})\cdot\hat{\mathbf{n}}$ is a continuous function of x_2 with values in $\mathbf{H}^{-1}((0,T)\times\mathbb{R})\otimes\mathbf{L}^2_\rho(\Gamma)$, and therefore, the restriction to $\{x_2 = 0\}$ is a well defined distribution. One can then employ the energy method and show that Theorem 1 also holds for the stochastic problem (1a)–(1b) with the boundary condition (13), see [30,31,24].

3.3.3. Absorbing boundary conditions

We now consider a boundary condition of the form

$$\mathbf{u}_t = M\,\boldsymbol{\sigma}(\mathbf{u})\cdot\hat{\mathbf{n}}, \tag{14}$$

where M is a given matrix in $\mathbb{R}^{d\times d}$ independent of $\mathbf{u}$. We assume that enough regularity is present so that the terms $\mathbf{u}_t$ and $\boldsymbol{\sigma}(\mathbf{u})\cdot\hat{\mathbf{n}}$ are well-defined on the boundary. With a negative definite matrix M, one can show that the boundary condition (14) results in a non-increasing energy (when $\mathbf{f} = \mathbf{0}$) and hence a well-posed problem (see, e.g., [35,36]). In a two-dimensional physical space, for instance, for a boundary given by $x_1 = 0$, a class of Clayton–Engquist boundary conditions is obtained by setting

$$M = -\begin{bmatrix} \dfrac{1}{\sqrt{\nu\,(2\,\mu+\lambda)}} & 0 \\ 0 & \dfrac{1}{\sqrt{\nu\,\mu}} \end{bmatrix}.$$

Such types of boundary conditions are called energy absorbing conditions. They are important in wave propagation problems, as they reduce the non-physical reflections of outgoing waves from artificial boundaries used to truncate the computational domain.

4. Stochastic regularity

In this section we study the regularity of the solution and some quantities of interest with respect to the random input variable Y under general assumptions on the data. As it will be shown, the Y-regularity is closely related to the regularity of data in time and space. The ultimate use of Y-regularity in obtaining convergence rate of the error for the stochastic collocation method will be discussed in the next section.

4.1. Stochastic regularity of the solution

Let us now consider more general assumptions on the regularity of the data than the assumption (3), namely,

$$\mathbf{f} \in \mathbf{L}^2((0,T);\mathbf{H}^s(D)), \qquad \mathbf{g}_1 \in \mathbf{H}^{s+1}(D), \qquad \mathbf{g}_2 \in \mathbf{H}^s(D), \qquad s \geq -1, \tag{15}$$

where s is an integer. Recall that we also assume that the initial data and external forcing are compactly supported inside D and that the final time T and the domain D are selected so that the wave solution $\mathbf{u}$ does not reach the boundary ∂D. Hence the displacement vector $\mathbf{u}$ will remain zero on the boundary for all $t \in [0,T]$ and all $Y \in \Gamma$. These assumptions will simplify the analysis in the physical space. In particular, the same regularity results will hold for the initial value problem (1a)–(1b) both in the whole space $\mathbb{R}^d$ (Cauchy problem) and in the bounded domain D augmented with either (1c) or (4). Note that the assumption (3) is a particular case of (15) with $s = 0$.

The definition of the weak solution for the stochastic IBVP (1) stated in Definition 1 is only for the case when $s = 0$. In a similar way, we can extend the definition of the weak solution for (1) under the general assumption (15) with $s \geq -1$. Alternatively, we can first view the solution $\mathbf{u}(t,\mathbf{x},Y)$ as a function of Y (see also Remark 1):

$$\mathbf{u} = \mathbf{u}(Y) : \Gamma \to \mathbf{C}^0([0,T];\mathbf{H}^{s+1}(D)),$$

and then introduce weak solutions based on such functions. Here, we follow the latter and define the notion of weak solutions to the stochastic IBVP (1) under the general assumption (15). We distinguish two different cases: the case when $s \geq 0$; and the low regular case when $s = -1$.

Definition 2. For the stochastic IBVP (1) with the data satisfying (15), with $s \geq 0$, and the coefficients satisfying (5)–(8), the function

$$\mathbf{u} = \mathbf{u}(Y) : \Gamma \to \mathbf{C}^0([0,T]; \mathbf{H}^{s+1}(D)) \cap \mathbf{C}^1([0,T]; \mathbf{H}^s(D)) \cap \mathbf{H}^2((0,T); \mathbf{H}^{s-1}(D)), \quad s \geq 0, \tag{16}$$

is a weak solution provided the following hold for every $Y \in \Gamma$:

(i) $\mathbf{u}(Y)\big|_{t=0} = \mathbf{g}_1$ and $\mathbf{u}'(Y)\big|_{t=0} = \mathbf{g}_2$,

(ii) for all test functions $\mathbf{v} \in \mathbf{C}_0^\infty([0,T]; \mathbf{H}^1(D))$:

$$\int_{[0,T]\times D} \left(\nu\, \mathbf{u}'' \cdot \mathbf{v} + \nabla \mathbf{v} : \boldsymbol{\sigma}(\mathbf{u})\right) d\mathbf{x}\, dt = \int_{[0,T]\times D} \mathbf{f} \cdot \mathbf{v}\, d\mathbf{x}\, dt. \tag{17}$$

We note that with an abuse of notation, the differentiation symbols $'$ or $''$ always refer to differentiation with respect to time.

In the low regular case when $s = -1$, instead of (16), the corresponding weak solution is the function

$$\mathbf{u} = \mathbf{u}(Y) : \Gamma \to \mathbf{C}^0([0,T]; \mathbf{H}^{s+1}(D)) \cap \mathbf{C}^1([0,T]; \mathbf{H}^s(D)), \quad s = -1. \tag{18}$$

Moreover, the weak formulation (17) is interpreted in the *distributional* sense (see,e.g., [30]), namely

$$\int_{[0,T]\times D} \mathbf{u} \cdot \left(\nu\, \mathbf{v}'' - \nabla \cdot \boldsymbol{\sigma}(\mathbf{v})\right) d\mathbf{x}\, dt = \int_{[0,T]\times D} \mathbf{f} \cdot \mathbf{v}\, d\mathbf{x}\, dt + \int_D \left(-\nu\, \mathbf{g}_2 \cdot \mathbf{v}(0) + \nu\, \mathbf{g}_1 \cdot \mathbf{v}'(0)\right) d\mathbf{x}, \tag{19}$$

with the test functions $\mathbf{v} \in \mathbb{V}$, where

$$\mathbb{V} := \left\{\mathbf{v} \;\middle|\; \nu\, \mathbf{v}'' - \nabla \cdot \boldsymbol{\sigma}(\mathbf{v}) = \boldsymbol{\psi} \in \mathbf{L}^2((0,T); \mathbf{L}^2(D)), \mathbf{v}(T,.) = \mathbf{v}'(T,.) = \mathbf{0} \text{ a.e. in } D, \quad \boldsymbol{\sigma}(\mathbf{v}) \cdot \hat{\mathbf{n}}|_{\partial D} = \mathbf{0} \text{ a.e. in } [0,T]\right\}.$$

In particular, note that when $\mathbf{v} \in \mathbb{V}$, by (11) we have for every $Y \in \Gamma$,

$$\mathbf{v} \in \mathbf{C}^0([0,T]; \mathbf{H}^1(D)), \qquad \mathbf{v}' \in \mathbf{C}^0([0,T]; \mathbf{L}^2(D)), \qquad \mathbf{v}'' \in \mathbf{L}^2((0,T); \mathbf{H}^{-1}(D)),$$

and (19) is well defined. See [30] for more details.

We now state the main result on the time and space regularity of the corresponding weak solution:

Theorem 2. *Consider the stochastic IBVP (1) with data given by (15) and with random coefficients satisfying (5)–(8). Then there is a unique weak solution* $\mathbf{u}(.,Y)$ *for every* $Y \in \Gamma$*, where*

$$\mathbf{u}(.,Y) \in \mathbf{C}^0([0,T]; \mathbf{H}^{s+1}(D)) \cap \mathbf{C}^1([0,T]; \mathbf{H}^s(D)) \cap \mathbf{H}^2((0,T); \mathbf{H}^{s-1}(D)), \quad \text{where } s \geq 0, \tag{20}$$

and

$$\mathbf{u}(.,Y) \in \mathbf{C}^0([0,T]; \mathbf{H}^{s+1}(D)) \cap \mathbf{C}^1([0,T]; \mathbf{H}^s(D)), \quad \text{where } s = -1, \tag{21}$$

which is uniformly bounded in Γ *and depends continuously on the data.*

Proof. The proof is an easy extension of the proof of Theorem 23.2.2 in [32] which is for all $s \in \mathbb{R}$. We note that the proof in [32] is for Cauchy problems and can be applied to our initial–boundary value problem since we assume that the solution will not reach the boundary ∂D for all $t \in [0,T]$ and all $Y \in \Gamma$. □

In other words, the above theorem states that in the interior of the domain D, the solution $\mathbf{u}$ gains *one derivative* in space over the force term $\mathbf{f}$.

To study the Y-regularity of the solution, consider both weak and strong formulations. We first consider the weak formulation (17) and k-times differentiate it with respect to Y_n, with $1 \leq k \leq s+1$, (observe that this implies $s \geq 0$), and obtain

$$\int_{[0,T]\times D} \left(\nu\, \partial_{Y_n}^k \mathbf{u}'' \cdot \mathbf{v} + \nabla \mathbf{v} : \boldsymbol{\sigma}(\partial_{Y_n}^k \mathbf{u})\right) d\mathbf{x}\, dt = f^{(k)}(\mathbf{v}), \tag{22}$$

where $f^{(k)}$ is a linear functional of $\mathbf{v}$, given by, thanks to (9),

$$f^{(k)}(\mathbf{v}) := -k \int_{[0,T]\times D} \left(\partial_{Y_n} \nu\, \partial_{Y_n}^{k-1} \mathbf{u}'' \cdot \mathbf{v} + \nabla \mathbf{v} : \tilde{\boldsymbol{\sigma}}(\partial_{Y_n}^{k-1} \mathbf{u})\right) d\mathbf{x}\, dt, \tag{23}$$

with

$$\tilde{\boldsymbol{\sigma}}(\mathbf{w}) := (\partial_{Y_n} \lambda)\ \nabla \cdot \mathbf{w}\, I + (\partial_{Y_n} \mu)\ (\nabla \mathbf{w} + (\nabla \mathbf{w})^\top). \tag{24}$$

Observe that $\mathbf{v}$ and $\mathbf{f}$ are independent of Y.

The weak formulation (22)–(23) has a similar form to (17), with a slightly different right hand side. The term in the right hand side of (17), which is a linear functional of $\mathbf{v}$, is replaced by $f^{(k)}(\mathbf{v})$, which is also a linear functional of $\mathbf{v}$. Consequently, the regularity of the weak solution $\partial_{Y_n}^k \mathbf{u}$ to (22)–(23), which determines the stochastic regularity of $\mathbf{u}$, can be obtained by the regularity of the functional $f^{(k)}(\mathbf{v})$, and by employing Theorem 2.

We next consider the strong formulation (1) in the presence of high regular data, in particular when $s \geq 2$. We then k-times differentiate it with respect to Y_n, with $1 \leq k \leq s+1$, and obtain

$$\nu\, \partial_{Y_n}^k \mathbf{u}_{tt} - \nabla \cdot \boldsymbol{\sigma}(\partial_{Y_n}^k \mathbf{u}) = k\, \nabla \cdot \tilde{\boldsymbol{\sigma}}(\partial_{Y_n}^{k-1} \mathbf{u}) - k\, \partial_{Y_n} \nu\, \partial_{Y_n}^{k-1} \mathbf{u}_{tt} =: \mathbf{f}^{(k)}, \tag{25a}$$

$$\partial_{Y_n}^k \mathbf{u}(0, \mathbf{x}, Y) = \mathbf{0}, \qquad \partial_{Y_n}^k \mathbf{u}_t(0, \mathbf{x}, Y) = \mathbf{0}, \tag{25b}$$

$$\boldsymbol{\sigma}(\partial_{Y_n}^k \mathbf{u}) \cdot \hat{\mathbf{n}} = -k\, \tilde{\boldsymbol{\sigma}}(\partial_{Y_n}^{k-1} \mathbf{u}) \cdot \hat{\mathbf{n}} =: \mathbf{0}. \tag{25c}$$

We observe that the initial data vanish because $\mathbf{g}_1$ and $\mathbf{g}_2$ are independent of Y_n. The boundary data also vanish because the solution does not reach the boundary for all $t \in [0, T]$ and all $Y \in \Gamma$, and hence $\tilde{\boldsymbol{\sigma}}(\partial_{Y_n}^{k-1} \mathbf{u})\big|_{\partial D} = \tilde{\boldsymbol{\sigma}}(\mathbf{0}) = \mathbf{0}$. The IBVP (25) has a similar form to the IBVP (1) with different data. Consequently, the regularity of the solution $\partial_{Y_n}^k \mathbf{u}$ to (25), which determines the stochastic regularity of $\mathbf{u}$, can be obtained by the regularity of the force term $\mathbf{f}^{(k)}$ and by employing again Theorem 2.

Remark 2. The assumption on the linearity of the coefficients in Y, i.e. the assumption (9), is only for simplifying algebraic formulas and does not impose any restriction. In fact, since the coefficients are linear in Y, their second and higher Y-derivatives are zero. For nonlinear coefficients, the right hand sides of (22) and (25a), i.e. $f^{(k)}(\mathbf{v})$ and $\mathbf{f}^{(k)}$, may have additional terms, containing Y-derivatives of $\mathbf{u}$ of order less than $k-1$ and Y-derivatives of ν, λ, and μ of order up to k. Consequently, under the assumption (8), these additional terms do not affect the regularity. For instance, consider the weak form (22) for the case $k = 2$. The new right hand side of (22), say $\tilde{f}^{(2)}(\mathbf{v})$, reads

$$\tilde{f}^{(2)}(\mathbf{v}) = \int_{[0,T]\times D} \Big(-2 \left(\partial_{Y_n} \nu\, \partial_{Y_n} \mathbf{u}'' \cdot \mathbf{v} + \nabla \mathbf{v} : \tilde{\boldsymbol{\sigma}}(\partial_{Y_n} \mathbf{u}) \right) - \left(\partial_{Y_n}^2 \nu\, \mathbf{u}'' \cdot \mathbf{v} + \nabla \mathbf{v} : \hat{\boldsymbol{\sigma}}(\mathbf{u}) \right) \Big)\, d\mathbf{x}\, dt,$$

where

$$\hat{\boldsymbol{\sigma}}(\mathbf{w}) := (\partial_{Y_n}^2 \lambda)\ \nabla \cdot \mathbf{w}\, I + (\partial_{Y_n}^2 \mu)\ (\nabla \mathbf{w} + (\nabla \mathbf{w})^\top).$$

Therefore, thanks to (8), the additional terms do not reduce the regularity, and the regularity results that follow hold true for general coefficients satisfying (5)–(8).

We also observe the following divergence formula for integration by parts, which will be used in this section,

$$\int_D \mathbf{v} \cdot \nabla \cdot \boldsymbol{\sigma}(\mathbf{u})\, d\mathbf{x} = -\int_D \nabla \mathbf{v} : \boldsymbol{\sigma}(\mathbf{u})\, d\mathbf{x} = \int_D \mathbf{u} \cdot \nabla \cdot \boldsymbol{\sigma}(\mathbf{v})\, d\mathbf{x}. \tag{26}$$

Note that both $\mathbf{u}$ and $\boldsymbol{\sigma}(\mathbf{u}) \cdot \hat{\mathbf{n}}$ are zero on the boundary ∂D, and therefore not boundary terms are present in (26). We now prove the following main result on the Y-regularity of the solution.

Theorem 3. *For the solution of the stochastic IBVP (1) with data given by (15) and with random coefficients satisfying (5)–(8), we have for* $0 \leq k \leq s+1$,

$$\partial_{Y_n}^k \mathbf{u}(., Y) \in \mathbf{C}^0([0, T]; \mathbf{H}^{s+1-k}(D)), \quad \forall\, Y \in \Gamma, \tag{27}$$

and uniformly bounded in Γ.

Proof. The case $k = 0$ corresponds to Theorem 2. Now let $k \geq 1$. We use induction on $1 \leq k \leq s+1$.

Case $k = 1$. In this case $s \geq 0$. We consider three different cases: $s = 0$, $s = 1$, and $s \geq 2$.

First let $s = 0$. From (22)–(23), we have

$$\int_{[0,T]\times D} \nu\, \partial_{Y_n} \mathbf{u}'' \cdot \mathbf{v}\, d\mathbf{x}\, dt + \int_{[0,T]\times D} \nabla \mathbf{v} : \boldsymbol{\sigma}(\partial_{Y_n} \mathbf{u})\, d\mathbf{x}\, dt = f^{(1)}(\mathbf{v}), \tag{28}$$

with

$$f^{(1)}(\mathbf{v}) = -\int_{[0,T]\times D} \partial_{Y_n} \nu\, \mathbf{u}'' \cdot \mathbf{v}\, d\mathbf{x}\, dt - \int_{[0,T]\times D} \nabla \mathbf{v} : \tilde{\boldsymbol{\sigma}}(\mathbf{u})\, d\mathbf{x}\, dt. \tag{29}$$

The linear functional (29) is bounded in the $\mathbf{L}^2((0,T); \mathbf{H}^{-1}(D))$ norm:

$$\|f^{(1)}\|_{\mathbf{L}^2((0,T);\mathbf{H}^{-1}(D))} = \sup_{\mathbf{v}\in\mathbf{L}^2((0,T);\mathbf{H}^1(D))} \frac{|f^{(1)}(\mathbf{v})|}{\|\mathbf{v}\|_{\mathbf{L}^2((0,T);\mathbf{H}^1(D))}} < \infty,$$

due to (8) and (20) for $s = 0$ and noticing that $\tilde{\boldsymbol{\sigma}}(\mathbf{u})$, given by (24), is linear with respect to $\nabla \mathbf{u}$. Therefore, comparing (28) and (17) with $\mathbf{u}$ replaced by $\partial_{Y_n} \mathbf{u}$, and interpreting it in the distributional sense (19), with $\mathbf{u}$ replaced by $\partial_{Y_n} \mathbf{u}$, we can employ (21) in Theorem 2, with $\mathbf{u}$ replaced by $\partial_{Y_n} \mathbf{u}$, and obtain (27) for $k = 1$ and $s = 0$ uniformly in Γ.

Next let $s = 1$. It is enough to show that the functional (29) is bounded in the $\mathbf{L}^2((0,T);\mathbf{L}^2(D))$ norm. If this is the case, we can employ (20) in Theorem 2, with $\mathbf{u}$ replaced by $\partial_{Y_n}\mathbf{u}$ and s replaced by $s-1=0$ to obtain (27) for $k=1$ and $s=1$. For this purpose, we first assume $\mathbf{v} \in \mathbf{L}^2((0,T);\mathbf{C}_0^\infty(D))$. The first term in the right hand side of (29) is obviously bounded, thanks to (8) and since $\mathbf{u}'' \in \mathbf{L}^2((0,T);\mathbf{L}^2(D))$ by (20) for $s=1$. For the second term, we use (26) and write

$$-\int_{[0,T]\times D} \nabla\mathbf{v} : \tilde{\boldsymbol{\sigma}}(\mathbf{u})\, d\mathbf{x}\, dt = \int_{[0,T]\times D} \mathbf{v}\cdot\nabla\cdot\tilde{\boldsymbol{\sigma}}(\mathbf{u})\, d\mathbf{x}\, dt.$$

The term in the right hand side of the above expression is bounded since $\mathbf{u} \in \mathbf{C}^0([0,T];\mathbf{H}^2(D))$ by (20) for $s=1$, and due to the linearity of $\tilde{\boldsymbol{\sigma}}(\mathbf{u})$ with respect to $\nabla\mathbf{u}$. We have therefore

$$\sup_{\mathbf{v}\in\mathbf{L}^2((0,T);\mathbf{C}_0^\infty(D))} \frac{|f^{(1)}(\mathbf{v})|}{\|\mathbf{v}\|_{\mathbf{L}^2((0,T);\mathbf{C}_0^\infty(D))}} < \infty.$$

Now, since the space $\mathbf{L}^2((0,T);\mathbf{C}_0^\infty(D))$ is dense in $\mathbf{L}^2((0,T);\mathbf{L}^2(D))$, by the Hahn–Banach theorem, we can extend the linear functional $f^{(1)}(\mathbf{v})$ to the space $\mathbf{L}^2((0,T);\mathbf{L}^2(D))$, and with

$$\|f^{(1)}\|_{\mathbf{L}^2((0,T);\mathbf{L}^2(D))} = \sup_{\mathbf{v}\in\mathbf{L}^2((0,T);\mathbf{L}^2(D))} \frac{|f^{(1)}(\mathbf{v})|}{\|\mathbf{v}\|_{\mathbf{L}^2((0,T);\mathbf{L}^2(D))}} < \infty.$$

Finally, we let $s \geq 2$. In this case, since the data have high regularity, we can use the strong formulation (25) with the force term $\mathbf{f}^{(1)} = \nabla\cdot\tilde{\boldsymbol{\sigma}}(\mathbf{u}) - \partial_{Y_n}\nu\,\mathbf{u}_{tt}$ and zero initial and boundary data. By (20), we have $\mathbf{u}(.,Y) \in \mathbf{C}^0([0,T];\mathbf{H}^{s+1}(D))$ and $\mathbf{u}_{tt} \in \mathbf{L}^2((0,T);\mathbf{H}^{s-1}(D))$. Hence, noting that $\tilde{\boldsymbol{\sigma}}(\mathbf{u})$ is linear with respect to $\nabla\mathbf{u}$, we have

$$\mathbf{f}^{(1)} \in \mathbf{L}^2((0,T);\mathbf{H}^{s-1}(D)).$$

Therefore, by (20) in Theorem 2, with $\mathbf{u}$ replaced by $\partial_{Y_n}\mathbf{u}$ and s replaced by $s-1\geq 1$, we get (27) for $k=1$ and $s\geq 2$.

General case. We now assume that (27) holds for $1 \leq k = k_0 \leq s$. We want to show that it also holds for $2 \leq k = k_0+1 \leq s+1$, that is,

$$\partial_{Y_n}^{k_0+1}\mathbf{u}(.,Y) \in \mathbf{C}^0([0,T];\mathbf{H}^{s-k_0}(D)), \quad \forall\, Y \in \Gamma. \tag{30}$$

For this, we need first to show that for low regular cases the functional $f^{(k_0+1)}(\mathbf{v})$ is bounded with $\mathbf{L}^2((0,T);\mathbf{H}^{s-k_0-1}(D))$ norm and then employ Theorem 2 to arrive at (30). But this follows by the induction hypothesis and using the same approach as in the case when $k=1$, by considering two cases: when $s-k_0=0$, and when $s-k_0=1$.

For high regular cases, we need to show that the force term in the strong formulation (25) satisfy

$$\mathbf{f}^{(k_0+1)} \in \mathbf{L}^2((0,T);\mathbf{H}^{s-k_0-1}(D)), \tag{31}$$

and then employ Theorem 2 to arrive at (30). But (31) follows by the induction hypothesis and using the same approach as in the case when $k=1$, by considering the case $s-k_0\geq 2$. This completes the proof. □

We now consider the mixed Y-derivatives of the solution and state the following result.

Theorem 4. *For the solution of the stochastic IBVP (1) with data given by (15) and with random coefficients satisfying (5)–(8), we have for a multi-index $\mathbf{k}\in\mathbb{N}^N$ with $0\leq|\mathbf{k}|\leq s+1$,*

$$\partial_Y^{\mathbf{k}}\mathbf{u}(.,Y) := \frac{\partial^{|\mathbf{k}|}}{\partial_{Y_1}^{k_1}\cdots\partial_{Y_N}^{k_N}}\mathbf{u}(.,Y) \in \mathbf{C}^0([0,T];\mathbf{H}^{s+1-|\mathbf{k}|}(D)), \quad \forall\, Y\in\Gamma, \tag{32}$$

and uniformly bounded in Γ.

Proof. The proof is an easy generalization of the previous theorem, following also the arguments in the proof of Theorem 6 in [18]. □

Remark 3. The smoothness assumption in (5) may be relaxed to a weaker assumption. In fact, we can obtain the same regularity results stated in Theorems 2–4 with the coefficients ν, λ and μ belonging to $C^s(D)$ almost surely.

4.2. Stochastic regularity of quantities of interest

In practical applications, such as earthquake engineering and petroleum exploration, the data (e.g. force terms) are often not highly regular, and therefore the elastic wave solutions have low stochastic regularity. In this section, we consider two

types of quantities of interest, that are of practical importance, and show that they have high stochastic regularity, even in the presence of low regular data. Such quantities are the key for the merit of stochastic collocation in practical applications.

4.2.1. Mollified solutions

Consider the quantity of interest

$$\mathcal{Q}(Y) = \int_0^T \int_D \mathbf{u}(t, \mathbf{x}, Y) \cdot \boldsymbol{\phi}(\mathbf{x})\, d\mathbf{x}\, dt, \tag{33}$$

where $\mathbf{u}$ solves (1) and $\boldsymbol{\phi} \in \mathbf{H}_0^k(D)$ is a compactly supported vector-valued mollifier with $k \in \mathbb{N}$ being a non-negative integer. The quantity (33) is related to observables that measure local or global averages. We let the data in (1) satisfy (15) with $s \in \mathbb{N}$ and investigate the Y-regularity of (33).

We first introduce the *influence function* (or dual solution) $\boldsymbol{\varphi}$ associated to the quantity of interest, $\mathcal{Q}$, as the solution of the dual problem

$$\nu(\mathbf{x}, Y)\, \boldsymbol{\varphi}_{tt}(t, \mathbf{x}, Y) - \nabla \cdot \boldsymbol{\sigma}(\boldsymbol{\varphi}(t, \mathbf{x}, Y)) = \boldsymbol{\phi}(\mathbf{x}) \quad \text{in } [0, T] \times D \times \Gamma, \tag{34a}$$

$$\boldsymbol{\varphi}(T, \mathbf{x}, Y) = \mathbf{0}, \qquad \boldsymbol{\varphi}_t(T, \mathbf{x}, Y) = \mathbf{0} \quad \text{on } \{t = T\} \times D \times \Gamma, \tag{34b}$$

$$\boldsymbol{\sigma}(\boldsymbol{\varphi}(t, \mathbf{x}, Y)) \cdot \hat{\mathbf{n}} = \mathbf{0} \quad \text{on } [0, T] \times \partial D \times \Gamma. \tag{34c}$$

We note that this is a well-posed backward elastic equation with zero data at the final time T and a time-independent force term. As before, we assume that the final time T and the spatial domain D are selected so that the dual solution $\boldsymbol{\varphi}$ will never reach the boundary ∂D for all $t \in [0, T]$ and all $Y \in \Gamma$. By Theorems 2 and 3, the dual solution $\boldsymbol{\varphi}$ satisfies

$$\boldsymbol{\varphi}(., Y) \in \mathbf{C}^0([0, T]; \mathbf{H}^{k+1}(D)), \qquad \partial_{Y_n}^{k+1} \boldsymbol{\varphi}(., Y) \in \mathbf{C}^0([0, T]; \mathbf{L}^2(D)), \quad \forall\, Y \in \Gamma,$$

with uniform norms in Γ. We further note that, since the coefficients and data in (34) are time-independent, the above regularity results hold also for all time derivatives of $\boldsymbol{\varphi}$.

To study the Y-regularity of the quantity of interest, similar to Section 4.1, we can consider and differentiate both the weak formulation of (17) in the case of low regular data ($s = 0, 1$) and the strong formulation (1) in the case of high regular data ($s \geq 2$) and proceed as before.

We are now ready to prove the following result.

Theorem 5. *Let $k, s \in \mathbb{N}$ be two non-negative integers. Moreover, assume that $\boldsymbol{\phi} \in \mathbf{H}_0^k(D)$. Then, under the assumption (15) and for linear coefficients of type (9) satisfying (5)–(8), the Y-derivatives of the quantity of interest (33) are given by*

$$\begin{aligned} d_{Y_n}^{s+k+1} \mathcal{Q}(Y) = {} & C_{s,k} \int_0^T \int_D \nabla \partial_{Y_n}^k \boldsymbol{\varphi} : \tilde{\boldsymbol{\sigma}}(\partial_{Y_n}^s \mathbf{u})\, d\mathbf{x}\, dt \\ & + C_{s,k} \int_0^T \int_D \partial_{Y_n} \nu\, \partial_{Y_n}^k \boldsymbol{\varphi}_{tt} \cdot \partial_{Y_n}^s \mathbf{u}\, d\mathbf{x}\, dt \\ & + C_{s,k} \int_D \partial_{Y_n} \nu \left[\partial_{Y_n}^k \boldsymbol{\varphi}(0, \mathbf{x}, Y) \cdot \partial_{Y_n}^s \mathbf{g}_2(\mathbf{x}) - \partial_{Y_n}^k \boldsymbol{\varphi}_t(0, \mathbf{x}, Y) \cdot \partial_{Y_n}^s \mathbf{g}_1(\mathbf{x}) \right] d\mathbf{x}, \end{aligned} \tag{35}$$

where $C_{s,k} = \frac{-1}{k!} \prod_{\ell=1}^{k+1} (s + \ell)$.

Proof. To make the presentation lighter, we detail here only the case of smooth solutions and differentiate the strong formulation (1) assuming that all differential operations are well defined. The final result given in (35) still holds for rough solutions as well by a density argument. In fact, one can first regularize the data in the primal and dual problems and derive (35) for the solution of the regularized problems. Then one let the regularization parameter go to zero.

We s-times differentiate (1) with respect to Y_n, with $s \geq 0$, and thanks to (9) obtain,

$$\nu\, \partial_{Y_n}^s \mathbf{u}_{tt} - \nabla \cdot \boldsymbol{\sigma}(\partial_{Y_n}^s \mathbf{u}) = s \nabla \cdot \tilde{\boldsymbol{\sigma}}(\partial_{Y_n}^{s-1} \mathbf{u}) - s\, \partial_{Y_n} \nu\, \partial_{Y_n}^{s-1} \mathbf{u}_{tt} \quad \text{in } [0, T] \times D \times \Gamma, \tag{36a}$$

$$\partial_{Y_n}^s \mathbf{u}(0, \mathbf{x}, Y) = \partial_{Y_n}^s \mathbf{g}_1(\mathbf{x}), \qquad \partial_{Y_n}^k \mathbf{u}_t(0, \mathbf{x}, Y) = \partial_{Y_n}^s \mathbf{g}_2(\mathbf{x}) \quad \text{on } \{t = 0\} \times D \times \Gamma, \tag{36b}$$

$$\boldsymbol{\sigma}(\partial_{Y_n}^s \mathbf{u}) \cdot \hat{\mathbf{n}} = \mathbf{0}, \qquad \text{on } [0, T] \times \partial D \times \Omega, \tag{36c}$$

where $\tilde{\boldsymbol{\sigma}}$ is given by (24). Note that when we differentiate the boundary condition (1c), we obtain $\boldsymbol{\sigma}(\partial_{Y_n}^s \mathbf{u}) \cdot \hat{\mathbf{n}} = -s\, \tilde{\boldsymbol{\sigma}}(\partial_{Y_n}^{s-1} \mathbf{u}) \cdot \hat{\mathbf{n}}$. But since the solution does not reach the boundary and is zero on ∂D, the right hand side vanishes. Also note that $\partial_{Y_n}^s \mathbf{g}_1(\mathbf{x})$ and $\partial_{Y_n}^s \mathbf{g}_2(\mathbf{x})$ in (36b) are always zero, except for $s = 0$. We emphasize that as before, assumption (9) on the linearity of random parameters is only for simplification purposes and does not impose any restriction. We prove (35) by induction on $k \geq 0$.

Case $k = 0$. In this case, we $s+1$ times differentiate (33) with respect to Y_n and use (34a). We have for every $s \geq 0$,

$$\begin{aligned} d_{Y_n}^{s+1}\mathcal{Q}(Y) &= \int_0^T \int_D \partial_{Y_n}^{s+1}\mathbf{u} \cdot \boldsymbol{\phi}\, d\mathbf{x}\, dt \\ &= \int_0^T \int_D \partial_{Y_n}^{s+1}\mathbf{u} \cdot \left(\nu\, \boldsymbol{\varphi}_{tt} - \nabla \cdot \boldsymbol{\sigma}(\boldsymbol{\varphi})\right) d\mathbf{x}\, dt \\ &= \int_0^T \int_D \nu\, \partial_{Y_n}^{s+1}\mathbf{u} \cdot \boldsymbol{\varphi}_{tt}\, d\mathbf{x}\, dt - \int_0^T \int_D \boldsymbol{\varphi} \cdot \nabla \cdot \boldsymbol{\sigma}(\partial_{Y_n}^{s+1}\mathbf{u})\, d\mathbf{x}\, dt, \end{aligned} \tag{37}$$

where the last equality follows by the second equality in (26). Note that all boundary terms vanish since both primal and dual solutions, $\mathbf{u}$ and $\boldsymbol{\varphi}$, are zero on the boundary ∂D. We now use (36a) and write

$$\begin{aligned} d_{Y_n}^{s+1}\mathcal{Q}(Y) &= \int_0^T \int_D \nu\, \partial_{Y_n}^{s+1}\mathbf{u} \cdot \boldsymbol{\varphi}_{tt}\, d\mathbf{x}\, dt - \int_0^T \int_D \boldsymbol{\varphi} \cdot \left(\nu\, \partial_{Y_n}^{s+1}\mathbf{u}_{tt} - (s+1)\, \nabla \cdot \tilde{\boldsymbol{\sigma}}(\partial_{Y_n}^{s}\mathbf{u}) + (s+1)\, \partial_{Y_n}\nu\, \partial_{Y_n}^{s}\mathbf{u}_{tt}\right) d\mathbf{x}\, dt \\ &= \int_0^T \int_D \nu \left(\partial_{Y_n}^{s+1}\mathbf{u} \cdot \boldsymbol{\varphi}_{tt} - \boldsymbol{\varphi} \cdot \partial_{Y_n}^{s+1}\mathbf{u}_{tt}\right) d\mathbf{x}\, dt \\ &\quad - (s+1) \int_0^T \int_D \nabla\boldsymbol{\varphi} : \tilde{\boldsymbol{\sigma}}(\partial_{Y_n}^{s}\mathbf{u})\, d\mathbf{x}\, dt - (s+1) \int_0^T \int_D \partial_{Y_n}\nu\, \boldsymbol{\varphi} \cdot \partial_{Y_n}^{s}\mathbf{u}_{tt}\, d\mathbf{x}\, dt, \end{aligned}$$

where the last equality follows by the first equality in (26) with $\boldsymbol{\sigma}$ replaced by $\tilde{\boldsymbol{\sigma}}$. By integration by parts in t, the first integral term vanishes because of the homogeneous terminal conditions (34b) at $t = T$ and the homogeneous initial conditions (36b) at $t = 0$ (with s replaced by $s+1$). If we further employ integration by parts in t twice on the last integral term, we obtain

$$\begin{aligned} d_{Y_n}^{s+1}\mathcal{Q}(Y) &= -(s+1) \int_0^T \int_D \nabla\boldsymbol{\varphi} : \tilde{\boldsymbol{\sigma}}(\partial_{Y_n}^{s}\mathbf{u})\, d\mathbf{x}\, dt - (s+1) \int_0^T \int_D \partial_{Y_n}\nu\, \boldsymbol{\varphi}_{tt} \cdot \partial_{Y_n}^{s}\mathbf{u}\, d\mathbf{x}\, dt \\ &\quad - (s+1) \int_D \partial_{Y_n}\nu \left[\boldsymbol{\varphi} \cdot \partial_{Y_n}^{s}\mathbf{u}_t - \boldsymbol{\varphi}_t \cdot \partial_{Y_n}^{s}\mathbf{u}\right]_0^T d\mathbf{x} \\ &= -(s+1) \int_0^T \int_D \nabla\boldsymbol{\varphi} : \tilde{\boldsymbol{\sigma}}(\partial_{Y_n}^{s}\mathbf{u})\, d\mathbf{x}\, dt - (s+1) \int_0^T \int_D \partial_{Y_n}\nu\, \boldsymbol{\varphi}_{tt} \cdot \partial_{Y_n}^{s}\mathbf{u}\, d\mathbf{x}\, dt \\ &\quad + (s+1) \int_D \partial_{Y_n}\nu \left[\boldsymbol{\varphi}(0,\mathbf{x},Y) \cdot \partial_{Y_n}^{s}\mathbf{g}_2(\mathbf{x}) - \boldsymbol{\varphi}_t(0,\mathbf{x},Y) \cdot \partial_{Y_n}^{s}\mathbf{g}_1(\mathbf{x})\right] d\mathbf{x}. \end{aligned} \tag{38}$$

Note that the last term in (38) is zero for $s \geq 1$. Therefore, (35) follows for $k = 0$.

General case $k \geq 1$. We assume that (35) holds for every $s \geq 0$ and $0 \leq k \leq K$ and show that

$$\begin{aligned} d_{Y_n}^{s+K+2}\mathcal{Q}(Y) &= C_{s,K+1} \int_0^T \int_D \nabla\partial_{Y_n}^{K+1}\boldsymbol{\varphi} : \tilde{\boldsymbol{\sigma}}(\partial_{Y_n}^{s}\mathbf{u})\, d\mathbf{x}\, dt \\ &\quad + C_{s,K+1} \int_0^T \int_D \partial_{Y_n}\nu\, \partial_{Y_n}^{K+1}\boldsymbol{\varphi}_{tt} \cdot \partial_{Y_n}^{s}\mathbf{u}\, d\mathbf{x}\, dt \\ &\quad + C_{s,K+1} \int_D \partial_{Y_n}\nu \left[\partial_{Y_n}^{K+1}\boldsymbol{\varphi}(0,\mathbf{x},Y) \cdot \partial_{Y_n}^{s}\mathbf{g}_2(\mathbf{x}) - \partial_{Y_n}^{K+1}\boldsymbol{\varphi}_t(0,\mathbf{x},Y) \cdot \partial_{Y_n}^{s}\mathbf{g}_1(\mathbf{x})\right] d\mathbf{x}. \end{aligned} \tag{39}$$

We first differentiate the induction hypothesis (35) for $k = K$ with respect to Y_n and get

$$\begin{aligned} d_{Y_n}^{s+K+2}\mathcal{Q}(Y) &= C_{s,K} \int_0^T \int_D \nabla\partial_{Y_n}^{K+1}\boldsymbol{\varphi} : \tilde{\boldsymbol{\sigma}}(\partial_{Y_n}^{s}\mathbf{u})\, d\mathbf{x}\, dt + C_{s,K} \int_0^T \int_D \nabla\partial_{Y_n}^{K}\boldsymbol{\varphi} : \tilde{\boldsymbol{\sigma}}(\partial_{Y_n}^{s+1}\mathbf{u})\, d\mathbf{x}\, dt \\ &\quad + C_{s,K} \int_0^T \int_D \partial_{Y_n}\nu\, \partial_{Y_n}^{K+1}\boldsymbol{\varphi}_{tt} \cdot \partial_{Y_n}^{s}\mathbf{u}\, d\mathbf{x}\, dt + C_{s,K} \int_0^T \int_D \partial_{Y_n}\nu\, \partial_{Y_n}^{K}\boldsymbol{\varphi}_{tt} \cdot \partial_{Y_n}^{s+1}\mathbf{u}\, d\mathbf{x}\, dt \\ &\quad + C_{s,K} \int_D \partial_{Y_n}\nu \left[\partial_{Y_n}^{K+1}\boldsymbol{\varphi}(0,\mathbf{x},Y) \cdot \partial_{Y_n}^{s}\mathbf{g}_2(\mathbf{x}) - \partial_{Y_n}^{K+1}\boldsymbol{\varphi}_t(0,\mathbf{x},Y) \cdot \partial_{Y_n}^{s}\mathbf{g}_1(\mathbf{x})\right] d\mathbf{x}. \end{aligned} \tag{40}$$

Notice that $\partial_{Y_n}^{s}\mathbf{g}_1(\mathbf{x})$ and $\partial_{Y_n}^{s}\mathbf{g}_2(\mathbf{x})$ are always zero, except for $s = 0$. Next, we note that the hypothesis holds also for $s+1$ and $k = K$,

$$d_{Y_n}^{s+K+2}\mathcal{Q}(Y) = C_{s+1,K} \int_0^T \int_D \nabla\partial_{Y_n}^{K}\boldsymbol{\varphi} : \tilde{\boldsymbol{\sigma}}(\partial_{Y_n}^{s+1}\mathbf{u})\, d\mathbf{x}\, dt + C_{s+1,K} \int_0^T \int_D \partial_{Y_n}\nu\, \partial_{Y_n}^{K}\boldsymbol{\varphi}_{tt} \cdot \partial_{Y_n}^{s+1}\mathbf{u}\, d\mathbf{x}\, dt. \tag{41}$$

Using (40) and (41), we can eliminate the terms involving $\partial_{Y_n}^{s+1}u$ and obtain (39). This completes the proof. □

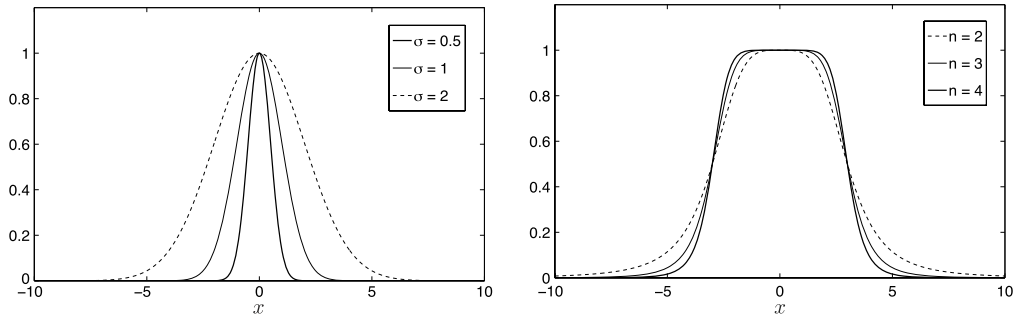

(a) $2\pi\sigma^2 K^G_\sigma$. (b) $K^B_{n,3}$.

Fig. 1. Transform functions for the one-dimensional Gaussian and Butterworth LPFs.

As a corollary of Theorem 5, we can write:

Corollary 1. *With the assumptions of Theorem 5, we have* $d^{s+k+1}_{Y_n}\mathcal{Q} \in L^\infty(\Gamma)$.

Similarly, we can study the mixed Y-derivatives of $\mathcal{Q}$.

Theorem 6. *Let* $k, s \in \mathbb{N}$ *be two non-negative integers. Moreover, assume that* $\boldsymbol{\phi} \in \mathbf{H}^k_0(D)$. *Then, under the assumption (15) and with random coefficients satisfying (5)–(8), we have* $d^{\mathbf{m}}_Y \mathcal{Q} \in L^\infty(\Gamma)$ *for a multi-index* $\mathbf{m} \in \mathbb{N}^N$ *with* $|\mathbf{m}| = s+k+1$. *In particular, when* $\boldsymbol{\phi} \in \mathbf{C}^\infty_0(D)$, *then* $\mathcal{Q} \in C^\infty(\Gamma)$.

Proof. The proof is similar to the proof of Theorem 5 by an easy modification of the technique used in [18] for the representation of mixed derivatives. □

4.2.2. Filtered solutions

In seismology and petroleum and gas industry, the simulated seismic data are often post-processed. One typical type of post-processing is filtering the data. For instance, a low-pass filter (LPF) is used in order to isolate and remove the high-frequency noise in the solution. In fact, the source time functions (see Section 6.2) trigger high frequency motions which are not resolvable on the mesh. The simulated solutions are therefore low-pass filtered and the high frequency errors are cut off. This is done by convolving the solution $u(t, \mathbf{x})$ with some smooth Kernels known as transfer functions. Two frequently used filters are Gaussian and Butterworth LPFs whose transfer functions read

$$K^G_\sigma(\mathbf{x}) = \frac{1}{2\pi\sigma^2} e^{-\frac{|\mathbf{x}|^2}{2\sigma^2}}, \qquad K^B_{n,r}(\mathbf{x}) = \frac{1}{\prod_{i=1}^{d}\left(1+(x_i/r)^{2n}\right)}, \tag{42}$$

respectively. In a Gaussian LPF, the standard deviation σ is inversely proportional to the maximum frequency that is allowed to pass. In a Butterworth LPF, the order n controls the sharpness of the cutoff, and r represents the frequency where the cutoff occurs. Fig. 1(a) shows the one-dimensional normalized Gaussian transfer function $2\pi\sigma^2 K^G_\sigma(x)$ for different values of σ, and Fig. 1(b) shows the one-dimensional Butterworth transfer function $K^B_{n,r}(x)$ with $r = 3$ and for different values of n. The value of r corresponds to the point where the Butterworth transfer function has value 1/2.

The filtered solution is then given by

$$\mathbf{u}^f(t, \mathbf{x}) = (\mathbf{u} \star K_\sigma)(t, \mathbf{x}) = \int_D K(\mathbf{x} - \tilde{\mathbf{x}})\, \mathbf{u}(t, \tilde{\mathbf{x}})\, d\tilde{\mathbf{x}}, \tag{43}$$

with the Kernel K given by either a Gaussian or a Butterworth transfer function in (42). We note that the filtered solution (43) is of a type similar to the quantity of interest (33). However, the main difference here is the boundary effects due to the convolution. Therefore, following the results of Sections 4.1 and 4.2.1, in the presence of a compactly supported smooth kernel $K \in C^\infty_0(D)$ as mollifier, the quantity (43) has high Y-regularity in the regions away enough from the boundary ∂D for which the support of $K(\mathbf{x}-\tilde{\mathbf{x}})$ does not cross the boundary ∂D. Although the smooth kernels given by (42) are not compactly supported, as we notice in Fig. 1, for small values of σ in the Gaussian filter and for large values of n and small values of r in the Butterworth filter, the kernels may be considered as *essentially* compactly supported. Hence, for such Gaussian and Butterworth LPFs, the filtered solution in points away from the boundary behaves as a quantity of interest with high Y-regularity. We refer to the test 2 in Section 6 for a numerical verification of high Y-regularity of a smoothed solution by a Gaussian filter.

5. Stochastic collocation

The stochastic collocation method consists of three main steps. First, the problem (1) is discretized in space and time, using a deterministic numerical method, such as the finite element or the finite difference method. The obtained semi-discrete problem is then collocated in a set of η collocation points $\{Y^{(k)}\}_{k=1}^{\eta} \in \Gamma$ to compute the approximate solutions $u_h(t, \mathbf{x}, Y^{(k)})$. Finally, a global polynomial approximation $u_{h,p}$ is built upon those evaluations

$$u_{h,p}(t, \mathbf{x}, Y) = \sum_{k=1}^{\eta} u_h(t, \mathbf{x}, Y^{(k)})\, L_k(Y),$$

for suitable multivariate polynomials $\{L_k\}_{k=1}^{\eta}$ such as Lagrange polynomials. Here, h and p represent the discretization mesh size and the polynomial degree, respectively. For more details we refer to [9,12].

A key point in the stochastic collocation method is the choice of the set of collocation points $\{Y^{(k)}\}$, i.e. the type of computational grid in the N-dimensional stochastic space. A full tensor grid, based on Cartesian product of mono-dimensional grids, can only be used when the number of stochastic dimensions N is small, since the computational cost grows exponentially fast with N (*curse of dimensionality*). To clarify this, let $\ell \in \mathbb{N}$ be a non-negative integer, called the *level*. Moreover, for a given index $j \in \mathbb{N}$, let $p(j)$ be a polynomial degree. Typical choices of the function p include

$$p(j) = j, \tag{44}$$

and

$$p(j) = 2^j \quad \text{for } j > 0, \qquad p(0) = 0. \tag{45}$$

In the full tensor grid, in each direction we take all polynomials of degree at most $p(\ell)$, and therefore $(p(\ell)+1)^N$ grid points are needed.

Alternatively, sparse grids can reduce the curse of dimensionality. They were originally introduced by Smolyak for high dimensional quadrature and interpolation computations (see [37]). In the following we will briefly review and generalize the sparse grid construction.

Let $\mathbf{j} \in \mathbb{Z}_+^N$ be a multi-index containing non-negative integers. For a non-negative index j_n in $\mathbf{j}$, we introduce a sequence of one-dimensional polynomial interpolant operators $\mathcal{U}^{j_n} : C^0(\Gamma_n) \to \mathbb{P}_{p(j_n)}(\Gamma_n)$ on $p(j_n)+1$ suitable knots. With $\mathcal{U}^{-1} = 0$, we define the detail operator

$$\Delta^{j_n} := \mathcal{U}^{j_n} - \mathcal{U}^{j_n - 1}.$$

Finally, introducing a sequence of index sets $\mathcal{I}(\ell) \subset \mathbb{Z}_+^N$, the sparse grid approximation of $u : \Gamma \to V$ at level ℓ reads

$$u_\ell(., Y) = \mathcal{S}_{\mathcal{I}(\ell),N}[u](., Y) = \sum_{\mathbf{j} \in \mathcal{I}(\ell)} \bigotimes_{n=1}^{N} \Delta^{j_n}\,[u](., Y). \tag{46}$$

The statistical moments of the solution or some given quantities of interest are computed by the Gauss quadrature formula corresponding to each interplant operator for approximating integrals (see, e.g., [18]). We note that $V = \mathbf{C}^0((0,T); \mathbf{H}^{s+1}(D))$ as in (20), and the regularity of the mapping $\Gamma \to V$ is given by (27). Furthermore, in order for the sum (46) to have some telescopic properties, which are desirable, we impose an additional admissibility condition on the set $\mathcal{I}$ (see [38]). An index set $\mathcal{I}$ is said to be *admissible* if $\forall\, \mathbf{j} \in \mathcal{I}$,

$$\mathbf{j} - \mathbf{e}_n \in \mathcal{I} \quad \text{for } 1 \le n \le N,\ j_n \ge 1,$$

holds. Here, $\mathbf{e}_n$ is the nth canonical unit vector.

To fully characterize the sparse approximation (46), we need to provide the following:

- A level $\ell \in \mathbb{N}$ and a function $p(j)$ representing the relation between an index j and the number of points in the corresponding one-dimensional polynomial interpolation formula $\mathcal{U}^j$.
- A sequence of sets $\mathcal{I}(\ell)$.
- The family of points to be used, such as Gauss or Clenshaw–Curtis abscissas [39].

Typical examples of index sets include

1. Full tensor grid: $\mathcal{I}(\ell) = \{\mathbf{j} :\ \max_n j_n \le \ell\}$.
2. Total degree sparse grid: $\mathcal{I}(\ell) = \{\mathbf{j} :\ \sum_{n=1}^{N} j_n \le \ell\}$ with $p(j) = j$.
3. Hyperbolic cross sparse grid: $\mathcal{I}(\ell) = \{\mathbf{j} :\ \prod_{n=1}^{N} (j_n + 1) \le \ell + 1\}$ with $p(j) = j$.

We now briefly motivate the construction of the hyperbolic cross sparse grid based on a simple optimality argument. A rigorous optimal sparse grid construction will be addressed elsewhere.

Let the error associated to a sparse grid be $E_{\mathcal{S}} = \|u - \mathcal{S}_{\mathcal{I}(\ell),N}[u]\|_{V \otimes L^2_\rho(\Gamma)}$, and the work $W_{\mathcal{S}}$ be the number of collocation points in the grid. We aim at finding the optimal set of indices that minimizes the error with a total work smaller than or

equal to a given maximum work. For this purpose, we introduce the error and work contribution of a multi-index $\mathbf{j}$ as $E_{\mathbf{j}}$ and $W_{\mathbf{j}}$, respectively. We then define the profit of an index as $P_{\mathbf{j}} = E_{\mathbf{j}}/W_{\mathbf{j}}$, and choose the optimal set including the most profitable indices: $\mathcal{I}^*(\epsilon) = \{\mathbf{j} \in \mathbb{N}^N : P_{\mathbf{j}} \geq \epsilon\}$, with a given positive threshold $\epsilon > 0$ (see, e.g., [40–42,38]).

Deriving a rigorous bound for the error is not easy. We denote the norm of each detail from (46) by

$$E_{\mathbf{j}} = \|\mathcal{S}_{\mathcal{I}(\ell),N}[u] - \mathcal{S}_{\mathcal{I}(\ell)\setminus\mathbf{j},N}[u]\| = \left\| \bigotimes_{n=1}^{N} \Delta^{j_n}[u] \right\|, \tag{47}$$

where $\mathcal{I}(\ell)$ is any admissible index set containing $\mathbf{j}$ such that $\mathcal{I}(\ell)\setminus\mathbf{j}$ is still admissible. For a function u with $s \geq 1$ bounded mixed Y-derivatives, we have (see [18])

$$E_{\mathbf{j}} \leq C \prod_{n=1}^{N} p(j_n)^{-s},$$

where C depends on s, N, and the size of all mixed Y-derivatives of u, but is independent of p and ℓ. We simplify the bound by setting $C \equiv 1$. The work, for non-nested grids, can be defined as $W_{\mathbf{j}} = W_{\mathcal{I}(\ell)} - W_{\mathcal{I}(\ell)\setminus\mathbf{j}}$ and can be bounded by

$$W_{\mathbf{j}} \leq \prod_{n=1}^{N} (p(j_n) + 1). \tag{48}$$

We notice that the error contribution (47) of a multi-index $\mathbf{j}$ is always independent of the set $\mathcal{I}(\ell)$ to which the multi-index is added. However, the work associated to a multi-index $\mathbf{j}$ depends, in general, on the set $\mathcal{I}(\ell)$, except in the case of nested grids (see Remark 4). Therefore, for non-nested grids, (48) is only an upper bound of the work, independent of $\mathcal{I}(\ell)$.

We can now estimate the profit of each multi-index and build an optimal set

$$\mathcal{I}^*(\epsilon) = \left\{ \mathbf{j} \in \mathbb{N}^N : \frac{\prod_{n=1}^{N} p(j_n)^{-s}}{\prod_{n=1}^{N} (p(j_n) + 1)} \geq \epsilon \right\}.$$

Equivalently, for $\ell = 0, 1, \ldots$ and large $p(j_n)$, we have

$$\mathcal{I}^*(\ell) = \left\{ \mathbf{j} \in \mathbb{N}^N : \sum_{n=1}^{N} \log(p(j_n) + 1) \leq \ell \right\},$$

which is a hyperbolic cross grid. We refer to the numerical test 2 in Section 6 for a numerical verification of the advantage of using hyperbolic cross grids over total degree grids.

Remark 4. In the case of using Smolyak-type grids with nested points (45), we can obtain a sharper bound for the work:

$$W_{\mathbf{j}} = \prod_{n=1}^{N} (p(j_n) + 1 - p(j_n - 1) - 1) = \prod_{n=1}^{N} 2^{j_n - 1}.$$

In this case we will also get

$$E_{\mathbf{j}} \leq C \prod_{n=1}^{N} p(j_n)^{-s} = C \prod_{n=1}^{N} 2^{-j_n s} = C\, 2^{-s \sum_{n=1}^{N} j_n},$$

and therefore the set $\mathcal{I}^*(\ell) = \{\mathbf{j} \in \mathbb{N}^N : \sum_{n=1}^{N} j_n \leq \ell\}$ is optimal among nested grids for which $p(j) = 2^j$. Notice that this choice corresponds to the classical Smolyak construction.

6. Numerical experiments

In this section, we consider the IBVP (1) in a two dimensional rectangular domain $D = [-1, 1] \times [-2, 0]$. We numerically simulate the problem by the stochastic collocation method and study the convergence of the statistical moments of the solution $\mathbf{u}$, the linear quantity of interest (33), and the filtered solution (43) using a Gaussian low-pass filter.

The deterministic solver employs an explicit, second order accurate finite difference method which discretizes the PDEs in its second order form (see [43]). We note that an alternative approach is to first rewrite the second order system (1) as a larger system of first order equations and then discretize the new system. This approach however has the disadvantage of introducing auxiliary variables with their associated constraints and boundary conditions. This in turn reduces computational efficiency and accuracy (see [44,45]). In the stochastic space, we use collocation on a variety of sparse grids based on Gauss abscissas.

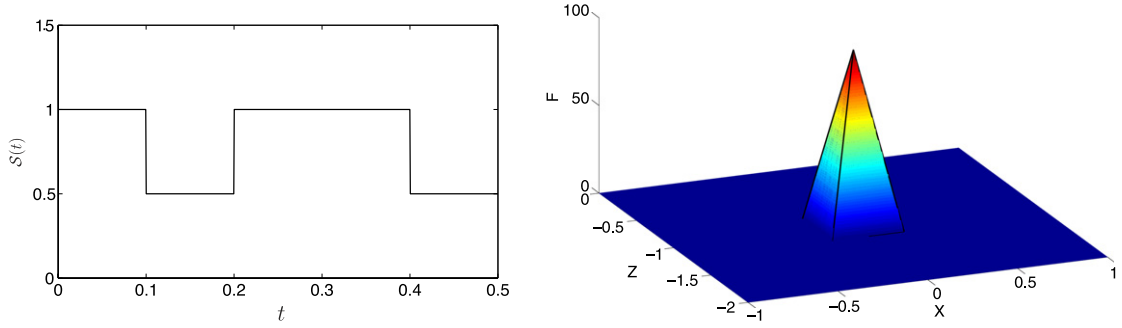

(a) $\mathcal{S} \in L^2(0,T)$. (b) $F \in H^1(D)$.

Fig. 2. Test 1. The force term $\mathbf{f} = (f_1, f_2)^\top$ given by $f_1 = f_2 = -\mathcal{S}(t)\,F(x,z)$.

We perform two numerical tests. In the first test, we consider a simple toy problem with a non-zero force term. In the second test, we simulate a simplified earthquake problem with slip on an extended fault surface. For both tests, we consider zero initial data $\mathbf{g}_1 = \mathbf{g}_2 = \mathbf{0}$ and apply a stress-free boundary condition (1c) at $z = 0$ and Clayton–Engquist non-reflecting boundary conditions (14) at the other three edges. We numerically study the convergence rate of the low-regular solution and high-regular quantities of interest.

6.1. Numerical test 1

In the first test, we consider a time-dependent force term $\mathbf{f} = (f_1, f_2)^\top$ with $f_1 = f_2 = -\mathcal{S}(t)\,F(x,z)$ inside $C = [-0.2, 0.2] \times [-1.2, -0.8]$, where

$$\mathcal{S}(t) = \begin{cases} 1, & t \in [0, 0.1) \cup [0.2, 0.4), \\ 0.5, & \text{otherwise}, \end{cases}$$

$$F(x,z) = \begin{cases} 500\,(0.2 - |x|), & \mathbf{x} \in C \text{ and } |z+1| \le |x|, \\ 500\,(0.2 - |z+1|), & \mathbf{x} \in C \text{ and } |z+1| > |x|, \\ 0, & \text{otherwise}. \end{cases}$$

Note that, with this choice, we have $\mathbf{f} \in \mathbf{L}^2((0,T); \mathbf{H}^1(D))$, see Fig. 2.

We consider the following $\mathbf{x}$-smooth random coefficients

$$\nu = 2.6, \qquad \mu = 2.5 + \cos\frac{4\pi\, z\, Y_1}{L_z} + \sin\frac{6\pi\, z\, Y_2}{L_z}, \qquad \lambda = 2\,\mu,$$

with two independent and uniformly distributed random variables $Y_n \sim \mathcal{U}(0.1, 0.5)$, $n = 1, 2$. Note that the above coefficients satisfy the assumptions (5)–(8).

We employ the collocation method on a hyperbolic cross sparse grid. We use a time step-size $\Delta t = \Delta x/4$ which guarantees the stability of the deterministic numerical solver. We study the convergence rate of the sparse grid collocation for two different choices of spatial grid-lengths $\Delta x = \Delta z = 0.05, 0.025$. For each grid-length $\Delta x = h$, we consider different levels $\ell \ge 1$ and compute the L^2-norm of error in the expected value of the solution on a part of the domain $D_0 \subset D$ at a fixed time $t = T$ by

$$\varepsilon_{\mathbf{u}} := \left(\int_{D_0} \left| \mathbb{E}\left[\mathbf{u}_{h,\ell}\right](T,\mathbf{x}) - \mathbb{E}\left[\mathbf{u}_{h,\ell_{\text{ref}}}\right](T,\mathbf{x}) \right|^2 d\mathbf{x} \right)^{1/2}. \tag{49}$$

Here, the reference solution $\mathbf{u}_{h,\ell_{\text{ref}}}$ is computed with a high level $\ell_{\text{ref}} > \ell$ for the same $\Delta x = h$. In this test, we choose $D_0 = D$ and $T = 0.5$.

We also compute the error in the expected value of the quantity of interest (33) at $T = 0.5$ by

$$\varepsilon_{\mathcal{Q}} := \left| \mathbb{E}\left[\mathcal{Q}[\mathbf{u}_{h,\ell}]\right] - \mathbb{E}\left[\mathcal{Q}[\mathbf{u}_{h,\ell_{\text{ref}}}]\right] \right|,$$

with a smooth mollifier $\boldsymbol{\phi} = (\phi_1, \phi_2)^\top \in \mathbf{C}_0^\infty(D)$, where

$$\phi_1(x,z) = \phi_2(x,z) = \begin{cases} 50\,\exp\left(\dfrac{0.32}{(x-0.4)^2 - 0.16} + \dfrac{0.32}{(z+0.4)^2 - 0.16} \right), & \mathbf{x} \in D_\phi \setminus \partial D_\phi, \\ 0, & \text{otherwise}, \end{cases}$$

with the support $D_\phi = [0, 0.8] \times [-0.8, 0] \subset D$.

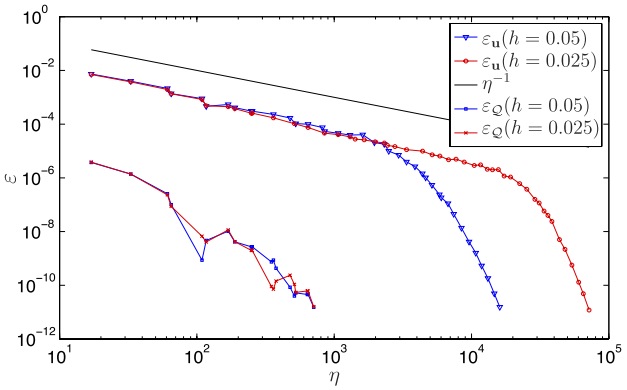

Fig. 3. Test 1. The L^2-norm of error in the expected value of the solution $\varepsilon_{\mathbf{u}}$ and the error in the expected value of the quantity of interest $\varepsilon_{\mathcal{Q}}$ at time $T = 0.5$ versus the number of collocation points $\eta(\ell)$. The solution has only two bounded Y-derivatives and one bounded mixed Y-derivative. However, the quantity of interest has bounded mixed Y-derivatives of any order and possesses high Y-regularity.

We note that since $\mathbf{f} \in \mathbf{L}^2(0, T; \mathbf{H}^1(D))$, by Theorem 3 for $s = 1$, we will have

$$\partial_{Y_n}^k \mathbf{u} \in \mathbf{L}^\infty(\Gamma; \mathbf{C}^0([0, T]; \mathbf{H}^{2-k}(D))), \quad 0 \le k \le 2.$$

Therefore, the solution has only two bounded Y-derivatives in $\mathbf{C}^0([0, T]; \mathbf{L}^2(D))$ and one bounded mixed Y-derivatives. Consequently, we expect a slow rate of error convergence for $\varepsilon_{\mathbf{u}}$. On the other hand, due to high Y-regularity of the quantity of interest, we expect a fast convergence rate for $\varepsilon_{\mathcal{Q}}$. Fig. 3 shows these two quantities versus the number of collocation points $\eta(\ell)$. We observe a slow convergence of order $\mathcal{O}(\eta^{-1})$ for $\varepsilon_{\mathbf{u}}$ and a faster convergence for $\varepsilon_{\mathcal{Q}}$, as expected. We also notice that for large values of $h\,\eta$, we observe exponential decay in the error $\varepsilon_{\mathbf{u}}$, and as h decreases, more collocation points are needed to maintain a fixed accuracy. In fact, as showed in [18], using the inverse inequality, we can show that the semi-discrete solution $\mathbf{u}_h$ can analytically be extended to a region in the complex plane with a radius proportional to h. Therefore, in building an approximate solution $\mathbf{u}_{h,\ell}$ to $\mathbf{u}_h$, we will observe a fast exponential decay in the error when the product $h\,\ell$ is large. Consequently, with a fixed h, the error convergence is slow (algebraic) for a small ℓ and fast (exponential) for a large ℓ. Moreover, the rate of convergence deteriorates as h gets smaller.

6.2. Numerical test 2

In the second test, we simulate a simplified earthquake problem with slip on an extended fault surface. We consider a two-dimensional problem which is similar to the three-dimensional problem LOH.2 defined by the Pacific Earthquake Engineering Center (see [46]).

In seismic wave propagation due to earthquakes and explosions, the source term is often composed of point sources (point moments) distributed over a fault surface,

$$\mathbf{f}(t, \mathbf{x}) = \sum_r \mathbf{f}_r^{(M)}(t, \mathbf{x}), \qquad \mathbf{f}_r^{(M)}(t, \mathbf{x}) = \mathcal{S}_r(t)\, \mathbf{M}_r\, \nabla\delta(\mathbf{x} - \mathbf{x}_r), \tag{50}$$

where $\mathcal{S}_r$ is the source time function, $\mathbf{M}_r$ is a constant symmetric matrix, and $\nabla\delta$ is the gradient of the Dirac distribution. Each term in (50) is applied at a location $\mathbf{x}_r = (x_r, z_r)$ which is independent of the grid $\mathbf{x}_{i,j}$. Based on the analysis of [47,48], it is possible to derive regularized approximations of the Dirac distribution and its gradient, which result in point-wise convergence of the solution away from the sources. The derivation of approximations of the Dirac distribution and its gradient is based on the following properties,

$$\int \phi(\mathbf{x})\, \delta(\mathbf{x} - \mathbf{x}_r)\, d\mathbf{x} = \phi(\mathbf{x}_r), \qquad \int \phi(\mathbf{x})\, \partial_x\delta(\mathbf{x} - \mathbf{x}_r)\, d\mathbf{x} = -\partial_x\phi(\mathbf{x}_r),$$

which holds for any smooth function ϕ. In one-dimension with a uniform grid x_k with grid size h, the integrals are replaced by a discrete scalar product $(p, q)_{1,h} := h \sum p_i\, q_i$. Cubic approximations of the Dirac distribution and its gradient are then obtained when the integral conditions are satisfied with ϕ being polynomials of degree three. Let $x_k \le x_r < x_{k+1}$ and $\alpha = (x_r - x_k)/h$. Then a third order discretization of $\delta(x - x_r)$ is given by

$$\delta_{k-1} = \frac{1}{h}\,(-\alpha/3 + \alpha^2/2 - \alpha^3/6),$$
$$\delta_k = \frac{1}{h}\,(1 - \alpha/2 - \alpha^2 + \alpha^3/2),$$
$$\delta_{k+1} = \frac{1}{h}\,(\alpha + \alpha^2/2 - \alpha^3/2),$$

$$\delta_{k+2} = \frac{1}{h}\,(-\alpha/6 + \alpha^3/6),$$
$$\delta_j = 0, \quad j \notin \{k-1, k, k+1, k+2\}.$$

Similarly, a third order discretization of $\delta'(x - x_r)$ is given by

$$\delta'_{k-1} = \frac{1}{h^2}\,(1/3 - \alpha + \alpha^2/2),$$
$$\delta'_k = \frac{1}{h^2}\,(1/2 + 2\,\alpha - 3\,\alpha^2/2),$$
$$\delta'_{k+1} = \frac{1}{h^2}\,(-1 - \alpha + 3\,\alpha^2/2),$$
$$\delta'_{k+2} = \frac{1}{h^2}\,(1/6 - \alpha^2/2),$$
$$\delta'_j = 0, \quad j \notin \{k-1, k, k+1, k+2\}.$$

For a two-dimensional problem, for instance, we then use

$$\delta(\mathbf{x} - \mathbf{x}_r) \approx \delta(x - x_r)\,\delta(z - z_r), \qquad \nabla\delta(\mathbf{x} - \mathbf{x}_r) \approx \begin{pmatrix} \delta'(x - x_r)\,\delta(z - z_r) \\ \delta(x - x_r)\,\delta'(z - z_r) \end{pmatrix}.$$

Using this representation, we obtain overall second order convergence of the solution away from the singularity at $\mathbf{x}_r$ (see [49]).

We model the slip on the extended fault by distributing point moment sources on a regular grid with size $\Delta s = 0.1$ (which is independent of the computational grid size $h = \Delta x = \Delta z$) over the fault surface given by $-0.3 \le x \le 0.1$, $-1.2 \le z \le -0.8$. The moment tensor in each source term is

$$\mathbf{M}_r = 7.5\,(\Delta s)^2 \begin{pmatrix} 1 & 0 \\ 0 & 0 \end{pmatrix}.$$

The earthquake starts at the hypo-center $\mathbf{x}_H = (-0.1, -1)$, and the rupture propagates along the fault surface with a uniform rupture velocity $c_{\text{rup}} = 1.7$. We use the source time function

$$\mathcal{S}_r(t) = \begin{cases} 0, & t < R_r/c_{\text{rup}}, \\ 1 - \left(1 + \dfrac{t - R_r/c_{\text{rup}}}{\tau}\right) e^{\frac{-(t - R_r/c_{\text{rup}})}{\tau}}, & t \ge R_r/c_{\text{rup}}, \end{cases}$$

where $\tau = 0.1$ is related to the rise time of the slip, and $R_r = |\mathbf{x}_r - \mathbf{x}_H|$. See Fig. 4. Based on this time function, each point source gets activated as soon as the rupture started from the hypo-center reaches the point source. We note that the size of the rise time τ is related to the frequency of the seismic waves it generates: the smaller the rise time, the higher the frequency.

We consider the following $\mathbf{x}$-smooth random coefficients of form (9)

$$\nu = 2.6, \qquad \mu = 1.5 + Y_1 + 0.15 \sum_{k=1}^{2} \left(Y_{2k} \cos \frac{2\,k\,\pi\,z}{L_z} + Y_{2k+1} \sin \frac{2\,k\,\pi\,z}{L_z} \right), \qquad \lambda = 2\,\mu,$$

where $Y_n \sim \mathcal{U}(0.1, 0.5)$, $n = 1, 2, \ldots, 5$, are five independent and uniformly distributed random variables.

We first employ the collocation method on a total degree sparse grid. We use a time step-size $\Delta t = \Delta x/4$ which guarantees the stability of the deterministic numerical solver. We compute the L^2-norm of error in the expected value of the solution (49) on $D_0 = [-1, 1] \times [-0.8, 0]$ at $T = 1$. We also compute the L^2-norm of error in the expected value of the filtered solution (43) at a fixed time $t = T$ by

$$\varepsilon_{\mathbf{u}^f} := \left(\int_{D_f} \left| \mathbb{E}\left[\mathbf{u}^f_{h,\ell} \right](T, \mathbf{x}) - \mathbb{E}\left[\mathbf{u}^f_{h,\ell_{\text{ref}}} \right](T, \mathbf{x}) \right|^2 d\mathbf{x} \right)^{1/2}, \tag{51}$$

over a window $D_f = [0.1, 0.2] \times [-1.1, -.9] \subset D$ away from the boundary ∂D. Here, the reference solution $\mathbf{u}^f_{h,\ell_{\text{ref}}}$ is again computed with a high level $\ell_{\text{ref}} > \ell$ on the same grid with $\Delta x = h$.

Fig. 5 shows the L^2-norm of error in the expected value of the solution $\varepsilon_{\mathbf{u}}$ and the error in the expected value of the filtered solution $\varepsilon_{\mathbf{u}^f}$ using a Gaussian Kernel K^G_σ in (42) with $\sigma = 2$ at $T = 1$ versus the number of collocation points $\eta(\ell)$. For the solution, there is no bounded Y-derivatives due to the presence of $\nabla\delta$ in the force term (50). We observe a slow convergence of order $\mathcal{O}(\eta^{-\delta})$ with $0 < \delta < 1/5$. On the other hand, for the filtered solution, we observe a fast convergence rate of order about $\mathcal{O}(\eta^{-3})$, which verifies that the filtered solution behaves as a quantity with high Y-regularity, as discussed in Section 4.2.2.

Next, we compare the performance of the collocation method on two different sparse grids; the total degree grid and the hyperbolic cross grid. Fig. 6 shows the L^2-norm of error in the expected value of the solution at $T = 1$ versus the number of collocation points $\eta(\ell)$ obtained by two different sparse grids. We clearly observe the advantage of using hyperbolic cross grids over total degree grids as predicted in Section 5.

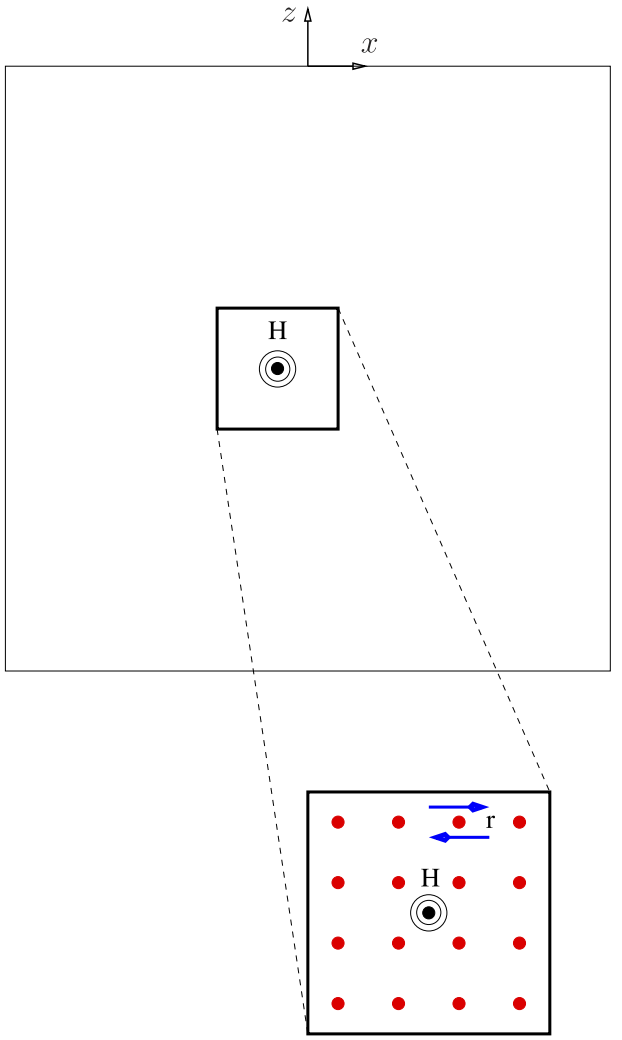

Fig. 4. Test 2. The computational domain and fault surface. The tick rectangle shows the fault surface, where the slip starts at the hypo-center indicated by concentric circles. Point moment sources are distributed on a regular grid on the fault surface.

7. Conclusions

We have analyzed the stochastic initial–boundary value problem for the elastic wave equation with random coefficients and deterministic data. We consider a random heterogeneous medium with time-independent and smooth material properties. We also assume that the wave length is not very small compared to the overall size of the domain and is comparable to the scale of the variations in the medium. We have studied the well-posedness and stochastic regularity of the problem by employing the energy method. We have also proposed a stochastic collocation method for computing statistical moments of the solution or some given quantities of interest and studied the convergence rate of the error.

The main result is that the stochastic regularity of the solution or the quantity of interest is closely related to the regularity of the deterministic data in the physical space and the type of the quantity of interest. We demonstrate that high stochastic regularity is possible in two cases: for the elastic wave solutions with high regular data; and for some high regular physical quantities of interest even in the presence of low regular data. For such problems, a fast spectral convergence is therefore possible when a stochastic collocation method is employed. We acknowledge that in practical applications, such as earthquake engineering and petroleum exploration, the data (e.g. force terms) are often not highly regular, and therefore the elastic wave solutions have low stochastic regularity. However, we have introduced several physical quantities with high stochastic regularity which may be of practical importance in such engineering fields. These quantities include *mollified quantities* (33), which are related to observables that are natural quantities for measuring local averages, and *filtered quantities* (43), which for instance are related to engineering quantities such as ground peak acceleration and spectral acceleration, obtained by performing a low-pass filter to isolate and remove the high-frequency noise in the solution. We stress here that we will need to solve the IBVP (1) far fewer times if we are after approximating such highly regular quantities

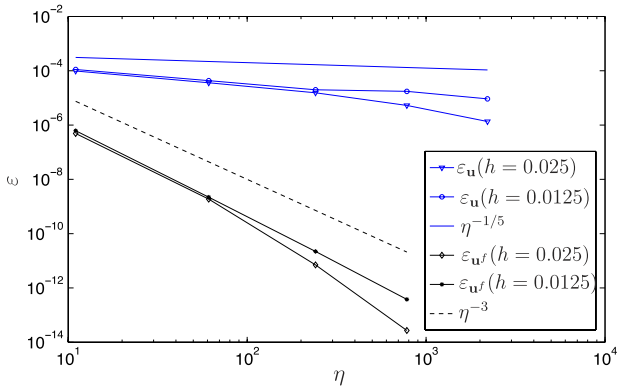

Fig. 5. Test 2. The L^2-norm of error in the expected value of the solution $\varepsilon_{\mathbf{u}}$ and the error in the expected value of the filtered solution $\varepsilon_{\mathbf{u}^f}$ at $T = 1$ versus the number of collocation points $\eta(\ell)$. The solution has no bounded Y-derivatives. However, the filtered solution behaves has a quantity with high Y-regularity.

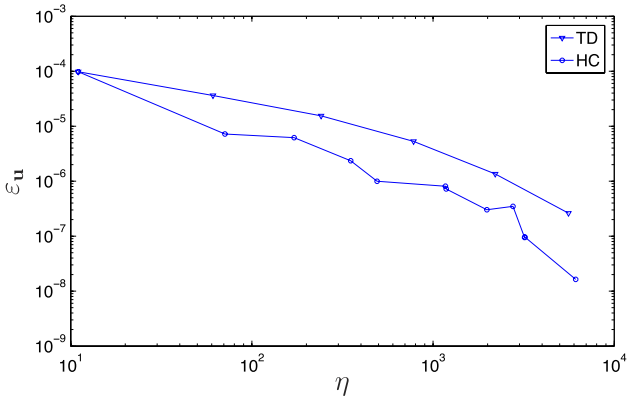

Fig. 6. Test 2. The L^2-norm of error in the expected value of the solution $\varepsilon_{\mathbf{u}}$ at time $T = 1$ versus the number of collocation points $\eta(\ell)$ computed on the total degree (TD) and the hyperbolic cross (HC) sparse grids.

of interest than when we are after approximating the wave solution $\mathbf{u}$ itself. The numerical examples presented in the paper are shown to be consistent with the analytical results and show that the stochastic collocation method is a valid alternative to the more traditional Monte Carlo method for approximating quantities with high stochastic regularity.

Acknowledgments

The authors would like to recognize the support of the PECOS center at ICES, University of Texas at Austin (Project Number 024550, Center for Predictive Computational Science). Support from the VR project "Effektiva numeriska metoder för stokastiska differentialekvationer med tillämpningar" and King Abdullah University of Science and Technology (KAUST) AEA project "Bayesian earthquake source validation for ground motion simulation" is also acknowledged. The third author is a member of the KAUST SRI Center for Uncertainty Quantification in Computational Science and Engineering. The second author has been supported by the Italian grant FIRB-IDEAS (Project n. RBID08223Z) "Advanced numerical techniques for uncertainty quantification in engineering and life science problems".

References

[1] G.S. Fishman, Monte Carlo: Concepts, Algorithms, and Applications, Springer-Verlag, New York, 1996.
[2] J. Dick, F.Y. Kuo, I.H. Sloan, High dimensional integration—the quasi-Monte Carlo way, Acta Numer. 22 (2013) 133–288.
[3] M.B. Giles, Multilevel Monte Carlo methods, Acta Numer. 24 (2015) 259–328.
[4] R.G. Ghanem, P.D. Spanos, Stochastic Finite Elements: A Spectral Approach, Springer, New York, 1991.
[5] H.G. Matthies, A. Kees, Galerkin methods for linear and nonlinear elliptic stochastic partial differential equations, Comput. Methods Appl. Mech. Engrg. 194 (2005) 1295–1331.
[6] D. Xiu, G.E. Karniadakis, Modeling uncertainty in steady state diffusion problems via generalized polynomial chaos, Comput. Methods Appl. Mech. Engrg. 191 (2002) 4927–4948.
[7] I. Babuska, R. Tempone, G.E. Zouraris, Solving elliptic boundary value problems with uncertain coefficients by the finite element method: the stochastic formulation, Comput. Methods Appl. Mech. Engrg. 194 (2005) 1251–1294.
[8] R.A. Todor, C. Schwab, Convergence rates for sparse chaos approximations of elliptic problems with stochastic coefficients, IMA J. Numer. Anal. 27 (2007) 232–261.

[9] I.M. Babuska, F. Nobile, R. Tempone, A stochastic collocation method for elliptic partial differential equations with random input data, SIAM J. Numer. Anal. 45 (2007) 1005–1034.
[10] F. Nobile, R. Tempone, C.G. Webster, An anisotropic sparse grid stochastic collocation method for partial differential equations with random input data, SIAM J. Numer. Anal. 46 (2008) 2411–2442.
[11] F. Nobile, R. Tempone, C.G. Webster, A sparse grid stochastic collocation method for partial differential equations with random input data, SIAM J. Numer. Anal. 46 (2008) 2309–2345.
[12] D. Xiu, J.S. Hesthaven, High-order collocation methods for differential equations with random inputs, SIAM J. Sci. Comput. 27 (2005) 1118–1139.
[13] F. Nobile, R. Tempone, Analysis and implementation issues for the numerical approximation of parabolic equations with random coefficients, Internat. J. Numer. Methods Engrg. 80 (2009) 979–1006.
[14] A. Cohen, R. DeVore, C. Schwab, Convergence rates of best N-term Galerkin approximations for a class of elliptic sPDEs, Found. Comput. Math. 10 (2010) 615–646.
[15] X. Wang, G.E. Karniadakis, Long-term behavior of ploynomial chaos in stochastic flow simulations, Comput. Methods Appl. Mech. Engrg. 195 (2006) 5582–5596.
[16] D. Gottlieb, D. Xiu, Galerkin method for wave equations with uncertain coefficients, Commun. Comput. Phys. 3 (2008) 505–518.
[17] T. Tang, T. Zhou, Convergence analysis for stochastic collocation methods to scalar hyperbolic equations with a random wave speed, Commun. Comput. Phys. 8 (2010) 226–248.
[18] M. Motamed, F. Nobile, R. Tempone, A stochastic collocation method for the second order wave equation with a discontinuous random speed, Numer. Math. 123 (2013) 493–536.
[19] G. Lin, C.-H. Su, G.E. Karniadakis, Predicting shock dynamics in the presence of uncertainties, J. Comput. Phys. 217 (2006) 260–276.
[20] G. Lin, C.-H. Su, G.E. Karniadakis, Stochastic modeling of random roughness in shock scattering problems: theory and simulations, Comput. Methods Appl. Mech. Engrg. 197 (2008) 3420–3434.
[21] G. Poette, B. Després, D. Lucor, Uncertainty quantification for systems of conservation laws, J. Comput. Phys. 228 (2009) 2443–2467.
[22] J. Tryoen, O. Le Maitre, M. Ndjinga, A. Ern, Intrusive projection methods with upwinding for uncertain nonlinear hyperbolic systems, J. Comput. Phys. 229 (2010) 6485–6511.
[23] J. Tryoen, O. Le Maitre, M. Ndjinga, A. Ern, Roe solver with entropy corrector for uncertain hyperbolic systems, J. Comput. Appl. Math. 235 (2010) 491–506.
[24] I. Lasiecka, R. Triggiani, Regularity theory of hyperbolic equations with non-homogeneous Neumann boundary conditions. II. General boundary data, J. Differential Equations 94 (1991) 112–164.
[25] I. Lasiecka, R. Triggiani, Recent advances in regularity of second-order hyperbolic mixed problems and applications, in: Dynamics Reported-Expositions in Dynamical Systems, Vol. 3, 1994, pp. 23–104.
[26] I. Babuska, M. Motamed, R. Tempone, A stochastic multiscale method for the elastodynamic wave equations arising from fiber composites, Comput. Methods Appl. Mech. Engrg. 276 (2014) 190–211.
[27] K.A. Cliffe, M.B. Giles, R. Scheichl, A.L. Teckentrup, Multilevel Monte Carlo methods and applications to elliptic PDEs with random coefficients, Comput. Vis. Sci. 14 (2011) 3–15.
[28] J. Charrier, Strong and weak error estimates for elliptic partial differential equations with random coefficients, SIAM J. Numer. Anal. 50 (2012) 216–246.
[29] H.-O. Kreiss, Initial boundary value problems for hyperbolic systems, Comm. Pure Appl. Math. 23 (1970) 277–298.
[30] J.L. Lions, E. Magenes, Non-homogeneous Boundary Value Problems and Applications I, Springer-Verlag, Berlin, 1972.
[31] J.L. Lions, E. Magenes, Non-homogeneous Boundary Value Problems and Applications II, Springer-Verlag, Berlin, 1972.
[32] L. Hörmander, The Analysis of Linear Partial Differential Operators III, Pseudo-Differential Operators, in: Classics in Mathematics, Springer, Berlin, 1994.
[33] L.C. Evans, Partial Differential Equations, in: Graduate Studies in Mathematics, vol. 19, American Mathematical Society, Providence, Rhode Island, 1998.
[34] C.C. Stolk, On the modeling and inversion of seismic data (Ph.D. thesis), Utrecht University, The Netherlands, 2000.
[35] R. Clayton, B. Engquist, Absorbing boundary conditions for acoustic and elastic wave equations, Bull. Seismol. Soc. Amer. 67 (1977) 1529–1540.
[36] N.A. Petersson, B. Sjögreen, An energy absorbing far-field boundary condition for the elastic wave equation, Commun. Comput. Phys. 6 (2009) 483–508.
[37] S.A. Smolyak, Quadrature and interpolation formulas for tensor products of certain classes of functions, Dokl. Akad. Nauk SSSR 4 (1963) 240–243.
[38] T. Gerstner, M. Griebel, Dimension-adaptive tensor-product quadrature, Computing 71 (2003) 65–87.
[39] L.N. Trefethen, Is Gauss quadrature better than Clenshaw–Curtis? SIAM Rev. 50 (2008) 67–87.
[40] J. Bäck, F. Nobile, L. Tamellini, R. Tempone, On the optimal polynomial approximation of stochastic PDEs by Galerkin and collocation methods, Math. Models Methods Appl. Sci. 22 (2012).
[41] M. Griebel, S. Knapek, Optimized general sparse grid approximation spaces for operator equations, Math. Comp. 78 (2009) 2223–2257.
[42] H.-J. Bungartz, M. Griebel, Sparse grids, Acta Numer. 13 (2004) 147–269.
[43] S. Nilsson, N.A. Petersson, B. Sjögren, H.-O. Kreiss, Stable difference approximations for the elastic wave equation in second order formulation, SIAM J. Numer. Anal. 45 (2007) 1902–1936.
[44] H.-O. Kreiss, O.E. Ortiz, Some mathematical and numerical questions connected with first and second order time-dependent systems of partial differential equations, Lecture Notes in Phys. 604 (2002) 359–370.
[45] H.-O. Kreiss, N.A. Petersson, J. Yström, Difference approximations for the second order wave equation, SIAM J. Numer. Anal. 40 (2002) 1940–1967.
[46] S.M. Day, J. Bielak, D. Dreger, S. Larsen, R. Graves, A. Ptarka, K.B. Olsen, Tests of 3D elastodynamic codes: Lifelines program task 1A01, Technical Report, Pacific Earthquake Engineering Center, 2001.
[47] J. Waldén, On the approximation of singular source terms in differential equations, Numer. Methods Partial Differential Equations 15 (1999) 503–520.
[48] A.-K. Tornberg, B. Engquist, Numerical approximation of singular source terms in differential equations, J. Comput. Phys. 200 (2004) 462–488.
[49] N.A. Petersson, B. Sjögreen, Stable grid refinement and singular source discretization for seismic wave simulations, Commun. Comput. Phys. 8 (2010) 1074–1110.